MATEMATICKO-FYZIKÁLNÍ FAKULTA
UNIVERZITY KARLOVY

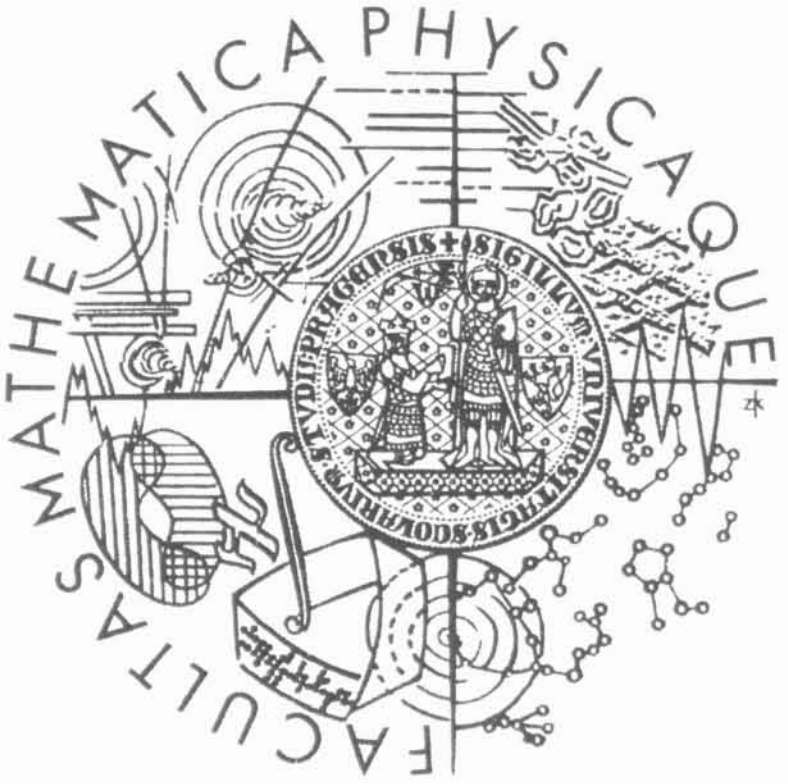

Zdeněk Lánský

Structural Properties of the H4-H5 loop of the Na^+/K^+ ATPase

Školitel: Doc. RNDr. Jaromír Plášek, CSc.
Konzultant: Doc. RNDr. Evžen Amler, CSc.

Obor: f-4 Biofyzika, chemická a makromolekulární fyzika
Školící pracoviště: Fyzikální ústav MFF UK a Fyziologický Ústav AVČR

Contents

Acknowledgement

First of all, I would like to express my gratitude to my supervisors, Doc. RNDr. Jaromír Plášek, CSc. and Doc. RNDr. Evžen Amler, CSc. for many valuable advices and suggestions concerning my experimental work and writing of this manuscript. My thanks also belong to RNDr. Martin Kubala, Ph.D. for a great help with many parts of this project, mainly the molecular biology and fluorescence experiments sections. I am also grateful to Ing. Jan Teisinger, CSc. for performing the protein mutagenesis and RNDr. Rüdiger Ettrich, Ph.D. for the molecular modelling and simulations.

Amino Acids Nomenclature

Amino Acid	One Letter Abbreviation	Three Letters Abbreviation
alanine	A	Ala
arginine	R	Arg
asparagine	N	Asn
aspartic acid	D	Asp
cysteine	C	Cys
glutamic acid	E	Glu
glutamine	Q	Gln
glycine	G	Gly
histidine	H	His
isoleucine	I	Ile
leucine	L	Leu
lysine	K	Lys
methionine	M	Met
phenylalanine	F	Phe
proline	P	Pro
serine	S	Ser
threonine	T	Thr
tryptophan	W	Trp
tyrosine	Y	Tyr
valine	V	Val
any amino acid	X	

Two following conventions are used within the text:

1) Number used with the amino acid abbreviation represents a position in the protein sequence, e.g., K501 or Lys^{501} denotes a lysine residue on the position 501.

2) Mutations are expressed by the one letter amino acid abbreviation, followed by a number and by a second one letter amino acid abbreviation. First letter denotes the original amino acid, the number its position in the protein sequence and last letter denotes the new amino acid, e.g., K501A denotes the substitution of the lysine residue on the position 501 for the alanine residue.

Abbreviations

2-azido-ATP	2-azidoadenosine 5'-triphosphate
8-azido-ATP	8-azidoadenosine 5'-triphosphate
ATP	adenosine 5'-triphosphate
ATPase	adenosine 5'-triphosphatase
BSA	bovine serum albumin
DNA	deoxyribonucleic acid
dNTP	mixture of deoxyribonuclotide 5'-triphosphates
DTT	DL-dithiothreitol
E1	conformation of P-type ATPases with high affinity to ATP
E2	conformation of P-type ATPases with low affinity to ATP
EDTA	ethylenediaminetetraacetic acid
FITC	fluorescein 5'-isothiocyanate
GST	glutathione-S-transferase from *Schistosoma japonicum*
H4-H5-loop	loop between the fourth and fifth transmembrane helices
IPTG	isopropyl-β-D-thiogalactoside
K605	wild-type sequence (Leu^{354}-Ile^{604}) of the Na^+/K^+-ATPase from mouse brain, fused with glutathione-S-transferase from *Schistosoma japonicum*
K_A	dissociation constant characterizing binding of ATP to the enzyme
K_D	dissociation constant
K_P	dissociation constant characterizing binding of fluorescent probe to the enzyme
LB medium	growth medium for bacteria according to Luria and Bertani
Na^+/K^+-ATPase	adenosine 5'-triphosphatase transporting sodium and potassium ions (other ATPases are designated analogously)
NMR	nuclear magnetic resonance
NP-40	tergitol, type NP-40
PCR	polymerase chain reaction
PDB	Protein Data Bank, http://www.rcsb.org/pdb/
PMSF	phenylmethanesulfonyl fluoride
SDS-PAGE	polyacrylamide gel electrophoresis, samples are denatured by sodium dodecyl sulphate
SERCA	Ca^{2+}-ATPase from sarco(endo)plasmic reticulum
TNP-ATP	2' (or 3')-O-(2,4,6-trinitrophenyl) adenosine 5'-triphosphate
WT	wild-type

1. Introduction

One of the most important issues every cell has to cope with is the transport of various chemical substances into and out of the cell. Full control over the composition of the cytoplasm is crucial for the proper functioning of every cellular process. Cells have evolved two major tools for its regulation: biological membrane that forms the impermeable barrier for many chemical compounds, and membrane transport proteins that can transport these compounds across the barrier into or out of the cytoplasm. Variability between the membrane transport proteins is huge and although these molecules were the subject of thorough examination for many years, a lot of their structural and functional features remain unclear.

In this work, we were interested in the protein transporting sodium and potassium ions across the plasma membrane called the Na^+/K^+ ATPase. We focused on the structure of one of its intracellular domains and, in particular, on the structure of the ATP binding site residing on this domain (Chapter 3).

The Na^+/K^+ ATPase belongs to the P-type ATPases family, which encompasses structurally and functionally similar membrane transport proteins (Chapter 2). One of the most intensively studied P-type ATPase is the calcium pump (Ca^{2+} ATPase). Recently, the structure of the Ca^{2+} ATPase from the sarco(endo)plasmatic reticulum (SERCA) was solved by the means of X-ray crystallography (Toyoshima 2000, 2002, 2004). Due to a high rate of homology between the calcium and sodium pump, these findings were very important for the construction of the molecular model of the Na^+/K^+ ATPase (Ettrich 2001) (Chapter 5).

In order to explore the structure of the Na^+/K^+ ATPase experimentally, several mutations were proposed on the basis of the molecular model (Chapter 6). These mutations were performed on the wild type (WT) sequence of the Na^+/K^+ ATPase, mutated protein constructs were expressed and purified (Chapter 6).

Steady state and time resolved fluorescence spectroscopy experiments were used to evaluate the influence of the mutations on the function of the Na^+/K^+ ATPase (Chapter 7). Ability to bind ATP was estimated for both, mutated and wild type constructs using the TNP-ATP, a fluorescent analog of ATP (Kubala 2003, 2004).

Results of fluorescence experiments were interpreted on the basis of the molecular model of the Na^+/K^+ ATPase. They are presented together with their

discussion in the Chapter 8, which is divided into three subchapters according to three main experimental areas of our project. The overall stability of the domain, where the ATP binding site resides (N-domain) is discussed in the Chapter 8.1. Number and precise position of ATP binding sites as well as the amino acid residues supporting the shape of the ATP binding pocket are discussed in Chapters 8.2 and 8.3. Short description of the currently running project which directly follows the ATP binding site study is in the Chapter 9. The presentation of achieved results in international journals is summarized in the Chapter 12.

2. P-type ATPases

Every living cell is isolated from its surroundings by a biological membrane, which is basically a fluid lipid bilayer that hosts a manifold of various membrane proteins. The lipid bilayer (Fig. 1) is impermeable for various polar reagents, e.g., ions, nutrients or toxins, due to its lipophilic character. However, these substances, for example toxins that should be expelled from the intracellular space, or ions that are essential for the maintenance of proper membrane potential, have to find their way across the membrane. For this purpose cells have evolved vast quantity of membrane proteins that transport different molecules into and out of cell. These proteins can be divided into two main categories. Channels, the first group, enable the flow of specific molecules in the direction of the concentration gradient. Pumps, on the other hand, work against the direction of the concentration gradient (Fig. 2) and therefore need some form of energy for this process. This energy comes often from the ATP hydrolysis. These proteins are thus denoted as ATPases.

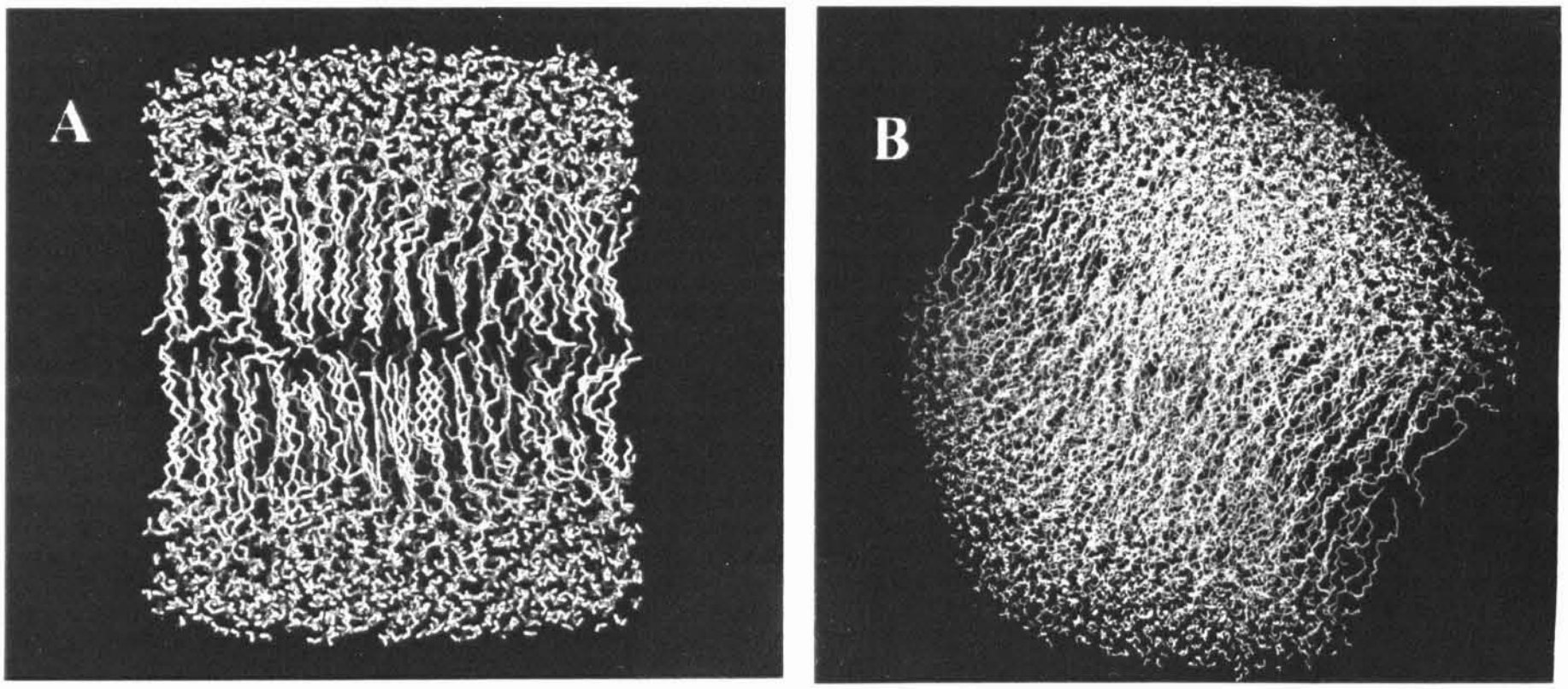

Fig. 1
Biological membrane – lipid bilayer.
(A) Viewing direction is parallel to the membrane. The hydrophobic tails are depicted in green, water molecules are depicted in red (oxygen) and white (hydrogen).
(B) 1-palmitoyl 2-oleoyl phosphatidyl choline bilayers (200 molecules total), hydrated with about 15 layers of water on each side (Heller 1993).

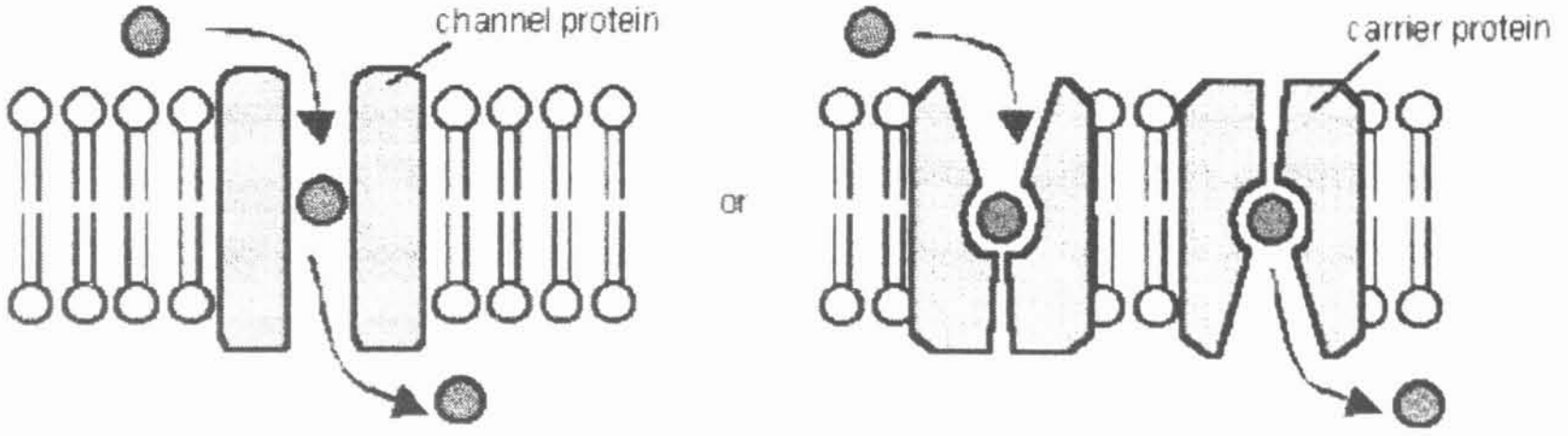

Fig. 2
Difference between the channel and the carrier (pump). (http://www.biologymad.com) Channel protein passively transports molecules in the direction of the concentration gradient. Carrier, on the other hand, uses energy to transport molecules actively across the plasma membrane.

Several hundreds of various transport ATPases with specificity for one or few substrates were identified. Based on particular structural similarities, they can be divided into three superfamilies (Kotyk 1998):

(1) multi-subunit enzymes anchored in the membrane by a special sector with a relatively large extramembrane cytoplasmic part (subtypes F and V),
(2) ATPases with two similar domains in the principal subunit (ABC subtype with a single subunit and Ars subtype with two subunits),
(3) ATPases with a single catalytically significant polypeptide containing a phosphorylation site (subtype P).

Na^+/K^+ ATPase, which has been the subject of our study, comes under the P subtype ATPases. The name P-ATPase comes from the observation of a transient phosphorylation during the catalytic cycle; the γ-phosphate of the ATP is transferred to the aspartate residue belonging to the phosphorylation site motif DKTGT present throughout the whole family. In 1998, Axelsen and Palmgren analyzed 211 sequences of P-type ATPases, and carried out further classification of these enzymes according to their substrate specificities (Fig. 3). According to their work, P – type ATPases can be divided into five main categories.

The first category includes bacterial K^+-ATPases, also denoted as Kdp-ATPases (Type IA) and ATPases transporting heavy metal ions, Cu^{2+} and Cd^{2+} (Type IB). The second category (Type II) is the largest one and can be further separated into several

subfamilies exhibiting various levels of conservation. Type IIA and Type IIB ATPases transport Ca^{2+}. Type IIC family contains closely related Na^+/K^+ and H^+/K^+-ATPases characteristic by the associated ~40kDa glycoprotein, designated as β-subunit. The co-translation association of the β-subunit is absolutely required for the maturation, targeting, stability, and functional expression of these proteins (Geering 2001). IIC P-ATPase α-subunit expressed in absence of the β-subunit exhibits no cation transport function. The last subfamily of the second category (Type IID) is formed by fungal ATPases. The third category encompasses H^+-ATPases (Type IIIA) and a small group of bacterial Mg^{2+}-ATPases (Type IIIB). The fourth category (Type IV) is formed by a family of enzymes found only in eukaryotes, some of which have been shown to be involved in the transport of aminophospholipids. ATPases having no assigned specificity form the fifth category (Type V) of this phylogenetic system (Fig. 3).

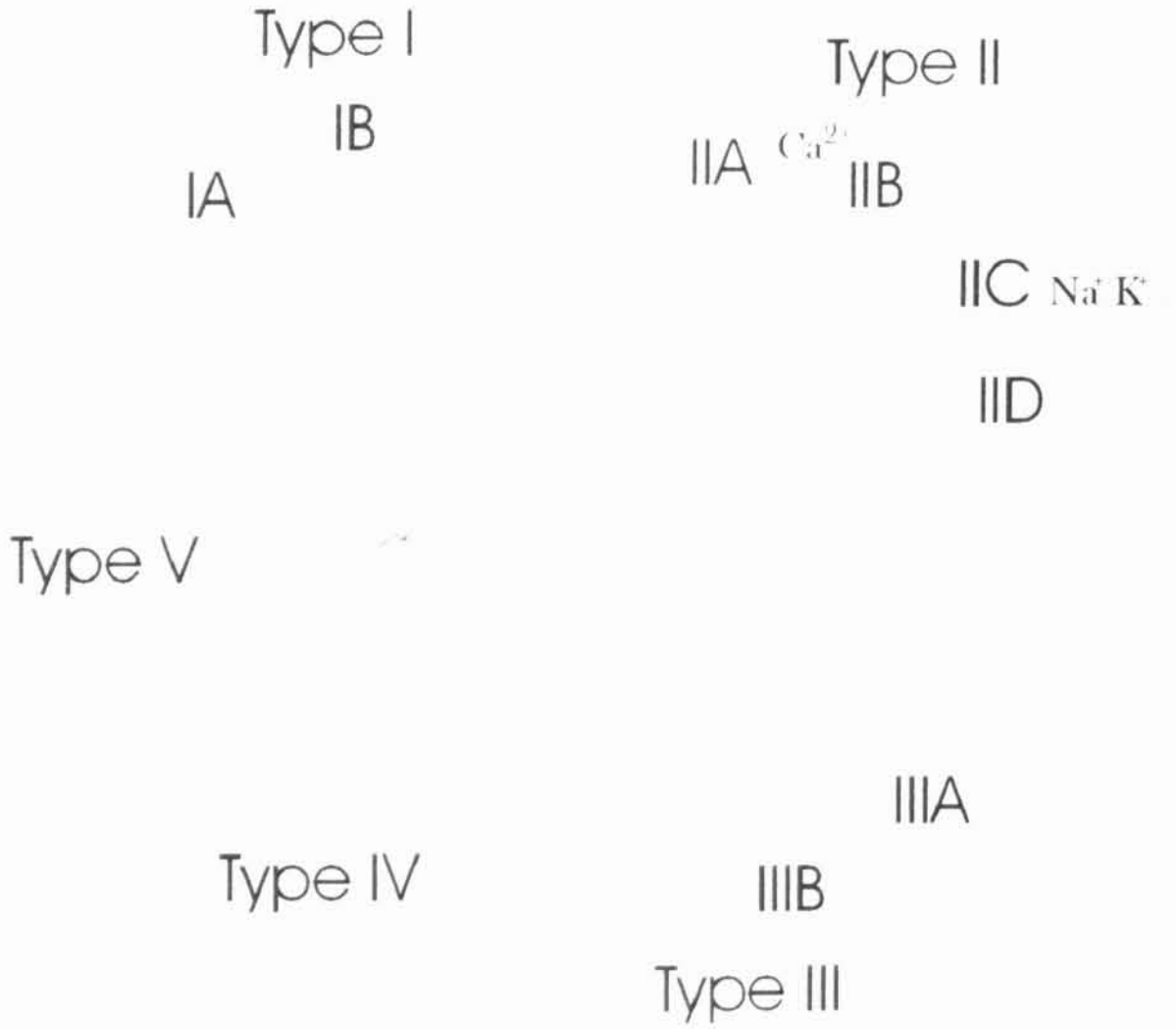

Fig. 3
P-type ATPase family phylogenetic tree.
This simplified and schematic tree with highlighted positions of the proteins of our interest, i.e. Na^+/K^+ ATPase and Ca^{2+} ATPase, represents the relationships between the main branches of the P-type ATPase family. Complete version of this tree can be found on the P-type ATPase Database internet site: http://biobase.dk/~axe/Patbase.html.

We have studied the ATPases of Type II, that have their catalytic subunit formed generally by 10 transmembrane helices, and during the catalytic cycle the subunit switches its conformation between two main conformational states. There are eight conserved sequence sections that define the core of P-type ATPases. These regions were identified, designated A-H and arranged in a linear sequence (Fig. 4). The largest percentage of homology is found on the large cytoplasmatic loop between the fourth and the fifth transmembrane segments (H4-H5 loop), where regions E-H reside. Region E contains the aspartyl residue, which is phosphorylated during the catalytic cycle. Furthermore, one can find another conserved sequence (designated I) on the H4-H5 loop, when the Type I ATPases are excluded (Moller 1996). Another highly conserved region is the loop connecting transmembrane helices 2 and 3, where the sequences A-C can be found. The only inter-membrane conserved region is the fourth transmembrane helix containing the sequence D.

Due to the structural and functional similarity of its members, the P-type ATPases family can be considered and explored collectively to a substantial extent. The results relating to one particular enzyme can be useful for the whole research within the P-type ATPases region of interest.

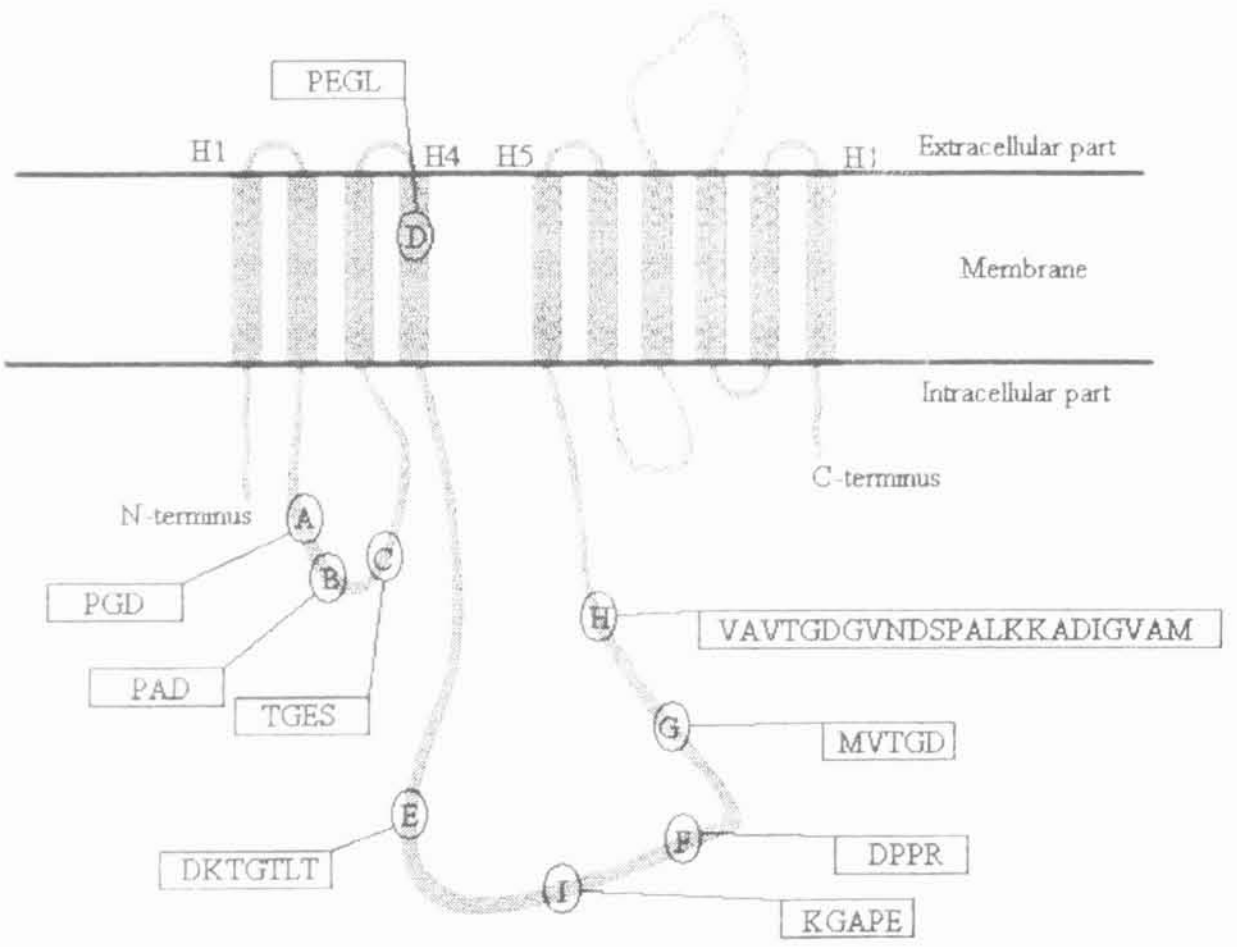

Fig. 4
An outline of the α-subunit of the P-type ATPase.
The conserved regions are designated A-H. One more conserved region (I) can be found, when the Type I ATPases are excluded. The phosphorylation site resides in the region E.

3. Na^+/K^+ ATPase

During the 5th decade of the previous century, many experimental works were carried out concerning the regulation and maintenance of the intracellular concentration of sodium and potassium ions (reviewed in Glynn 2002). This issue is very important because the gradients of these ions across the plasma membrane provide the energy for several essential cellular functions as e.g. control of the membrane potential, cell volume, pH homeostasis and many others. One of the greatest achievements of this experimental effort was the identification and isolation of the enzyme responsible for the active transport of the sodium and potassium ions across the plasma membrane, i.e. the Na^+/K^+ ATPase or the so called sodium pump (Skou 1957, 1960, 1962).

As the function of the Na^+/K^+ ATPase is rather crucial, it is not surprising that this membrane transport protein is present in cells of most higher eukaryotes. The Na^+/K^+ ATPase is a heterodimeric protein consisting of an α and β subunits present in the 1:1 stoichiometry. In some cases, for example when the enzyme is purified from kidneys, the α-β heterodimer is accompanied by another small protein; the γ-subunit. This optional subunit comes from the "FXYD" protein family, which has been recently identified and described (Sweadner 2000).

During the catalytic cycle the Na^+/K^+ ATPase comes through two main conformations (denoted E1 and E2) transporting three sodium ions out of the cell and two potassium ions into the cell. The enzyme works against a concentration gradient, and needs therefore a source of energy for its functioning. The energy for the completion of the transport cycle comes from the hydrolysis of a single ATP molecule.

3.1. Structure

3.1.1. α-subunit

The α-subunit of the Na^+/K^+ ATPase is composed of approximately 1000 amino acid residues and its molecular weight is approximately 110 kDa. Four distinct isoforms of the α-subunit have been identified. The sequence and functional differences among the isoforms are very small. However, the isoforms are unequally distributed in various tissues, representing their different physiological needs. The major α_1 form is found in most tissues and is the major in kidney and most epithelia. In cardiac tissue, different isoforms (α_1 and α_2), notably, have uneven distribution in different parts of a single cell. Tissue specifity is most significant in spermatozoa, where the α_4 form resides and its inhibition has been shown to eliminate sperm motility (Kaplan 2002).

Both N- and C- termini of the α-subunit of the Na^+/K^+ ATPase are localized on the intracellular side of the plasma membrane (Antolovic 1991). The number of membrane spanning segments, on the other hand, was the subject of many discussions. Three major hypotheses emerged, suggesting eight (Jorgensen 1988), nine (Dzandzhugazyan 1994) and ten (Moller 1996) membrane-spanning segments. Following many biochemical studies, a consensus of ten transmembrane segments appeared (Karlish 1993), although the final vindication of this idea came with the release of Ca^{2+} ATPase (Toyoshima 2000) crystallographic studies.

There are five very short extracellular loops (except for H7-H8 loop) and three main intracellular structures on the α-subunit (Fig. 4). These structures are long N-terminal tail (~90 amino acid residues), the H2-H3 loop (~120 amino acid residues) and the large H4-H5 loop composed of approximately 430 amino acid residues. Similarly as in the high resolution studies of Ca^{2+} ATPase (Toyoshima 2000), cryo-electron microscopy of Na^+/K^+ ATPase (Rice 2001) exhibited three major domains consisting of the large intracellular loops and the N-terminal tail. The N (nucleotide binding) and P (phosphorylation) domains resides on the H4-H5 loop, whereas the A (actuator) domain is formed by the amino-terminal tail and the H2-H3 loop.

One of the most striking discrepancies between the Na^+/K^+ ATPase and the Ca^{2+} ATPase is the large extracellular H7-H8 loop, which is significantly longer in Na^+/K^+ ATPase than in SERCA. This loop, and the sequence

^{894}NDVEDSYGQQWTFEQRKIVEFTCHTA^{919} in particular, was shown to form the important contact region with the associated β-subunit (Lemas 1994). Site directed mutational analysis aimed at the H7-H8 loop showed also the great importance of this region during the potassium ion transport (Schneider 1997). Another important characteristic is the position of binding sites for various inhibitors on the extracellular regions of the α-subunit. Some of these inhibitors are widely used in clinical medicine, for example for the treatment of the heart failure (Horisberger 2004). One of the most examined, highly specific and efficient inhibitor of the Na^+/K^+ ATPase is ouabain. When ouabain is bound to the Na^+/K^+ ATPase, the mutual movement of the membrane-spanning segments is blocked, hence disabling the transitions between conformational states of the Na^+/K^+ ATPase. This blocking results in the complete inability to transport sodium and potassium ions across the plasma membrane. Comparison of ouabain-sensitive and ouabain-resistant isoforms of the sodium pump, together with mutagenesis experiments pointed out several regions involved in the ouabain binding. The residues on H1-H2 loop that are directly in contact with ouabain are Gln111, Pro118, Asp121 and Asn122 (Kent 1987, Price 1990). Moreover, on the H3-H4 loop there is the Tyr308 and on the H7-H8 loop there is the Arg880 (Schultheis 1993).

Cation binding sites are formed by the membrane spanning helices, whose mutual movement during the transitions between the E1 and E2 conformation cause the uptake and release of the ions. Several mutational experiments were carried out to prove the exact position of the cation binding site. Effect of these mutations didn't always lead to significant changes of the cation affinity of the Na^+/K^+ ATPase and the results of this experimental work weren't much convincing (Vilsen 1993, 1995). This is probably due to the nature of the cation binding. The cations, as suggested by Scheiner-Bobis (2002), are coordinated by carbonyl groups along the backbone of the protein and their mutual interaction with the peptidic chain has rather an ion-dipole than an ion-ion character. High resolution Ca^{2+} ATPase structure might bring some more light upon this issue.

The crystal of SERCA has two clearly defined Ca^{2+} binding sites approximately at the middle of the membrane. Site I is located between transmembrane segments 5 and 6, and site II is formed by a short unfolded region of the transmembrane segment 4 and resides between the transmembrane segments 4 and 6 (Toyoshima 2000) (Fig. 5). As the stoichiometry of the Na^+/K^+ ATPase is $3Na^+$ / $2K^+$ / 1ATP, the enzyme should be able to provide three Na^+ binding sites. Ogawa and Toyoshima (2002) proposed that two sodium ions occupy two sites homologous to the I and II Ca^{2+} binding sites of SERCA. They also predicted the third binding site at the same level in the membrane, but closer to the transmembrane segment 9.

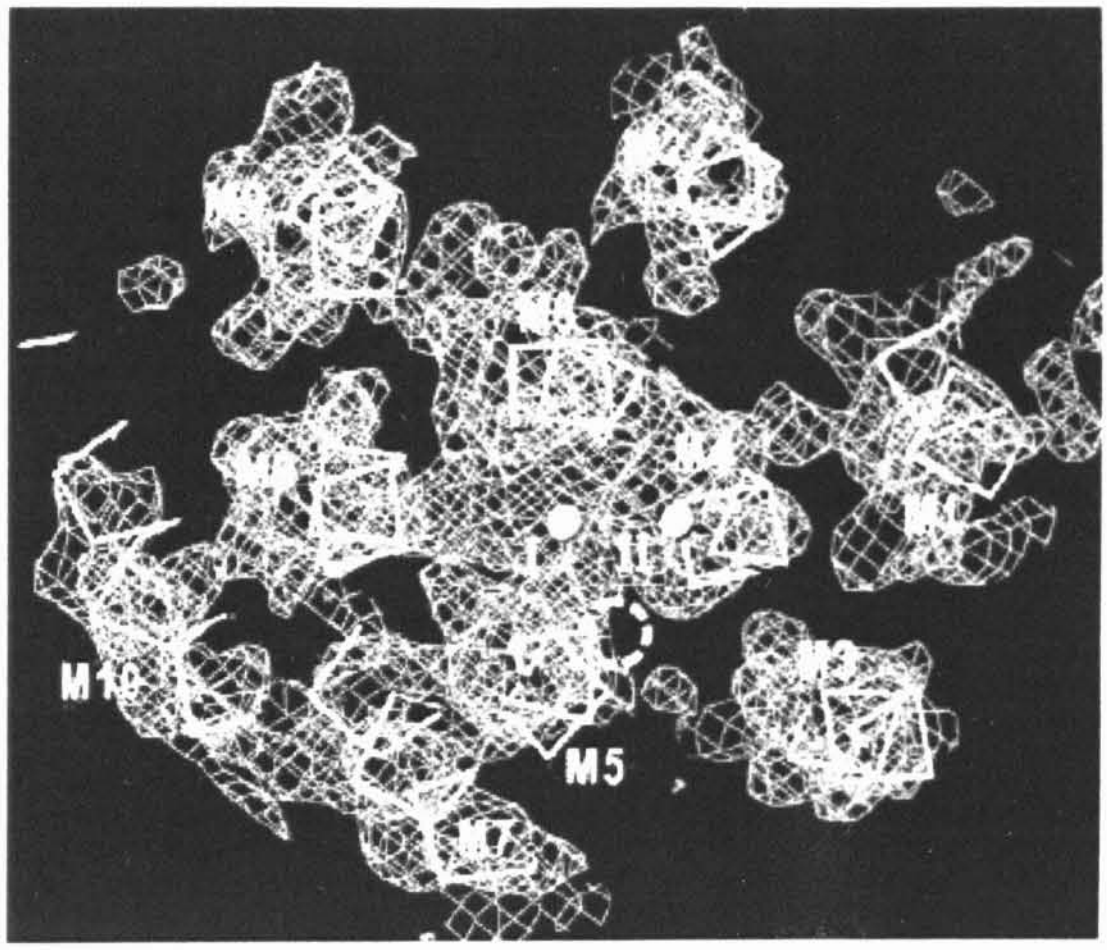

Fig. 5a
SERCA cation binding sites (Toyoshima 2000).
The viewing direction is normal to the membrane from the cytoplasmatic side with the A-domain on the right hand side. Cyan spheres represent the Ca^{2+} ions (I and II). The circle represents the likely position of the outlet of Ca^{2+} pathway.

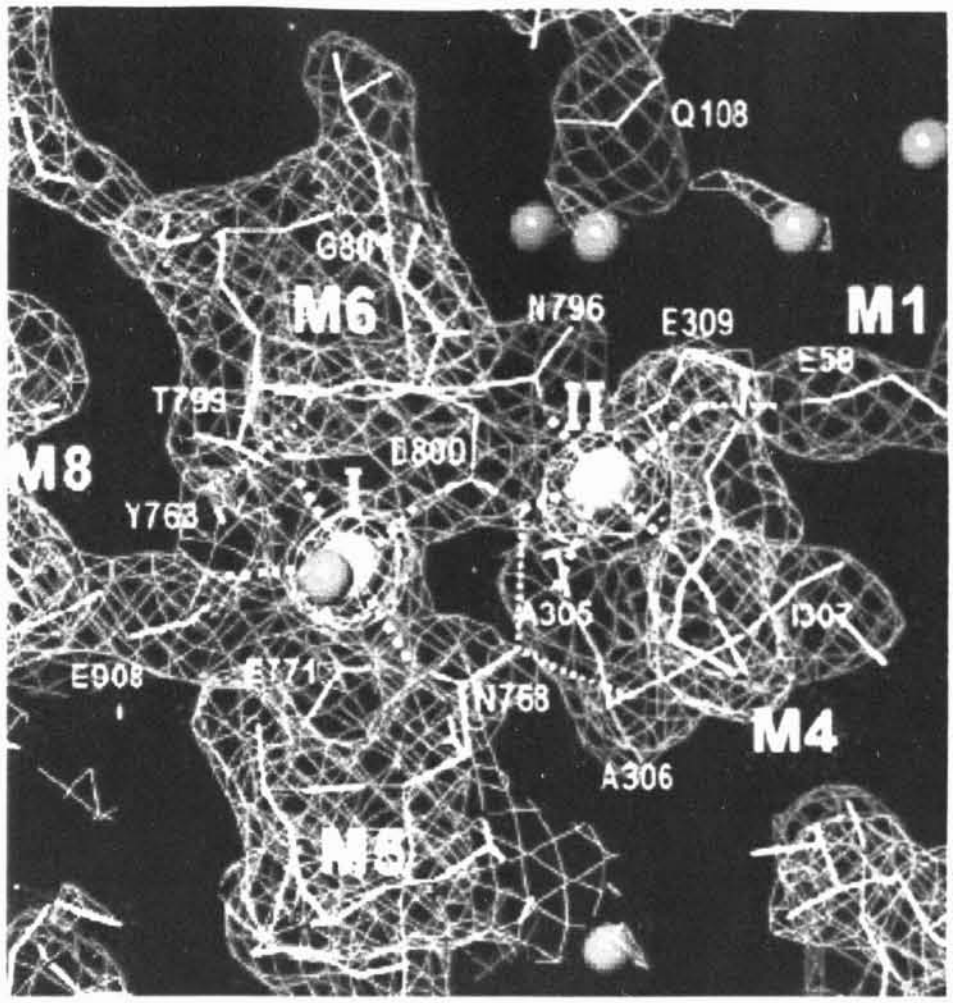

Fig. 5b
Detail of the transmembrane Ca^{2+} binding sites (Toyoshima 2000).
Cyan spheres represent the Ca^{2+} ions and red spheres represent the water molecules. The viewing direction is normal to the membrane from the cytoplasmatic site. The coordinations of oxygen atoms to Ca^{2+} are indicated by white dotted lines.

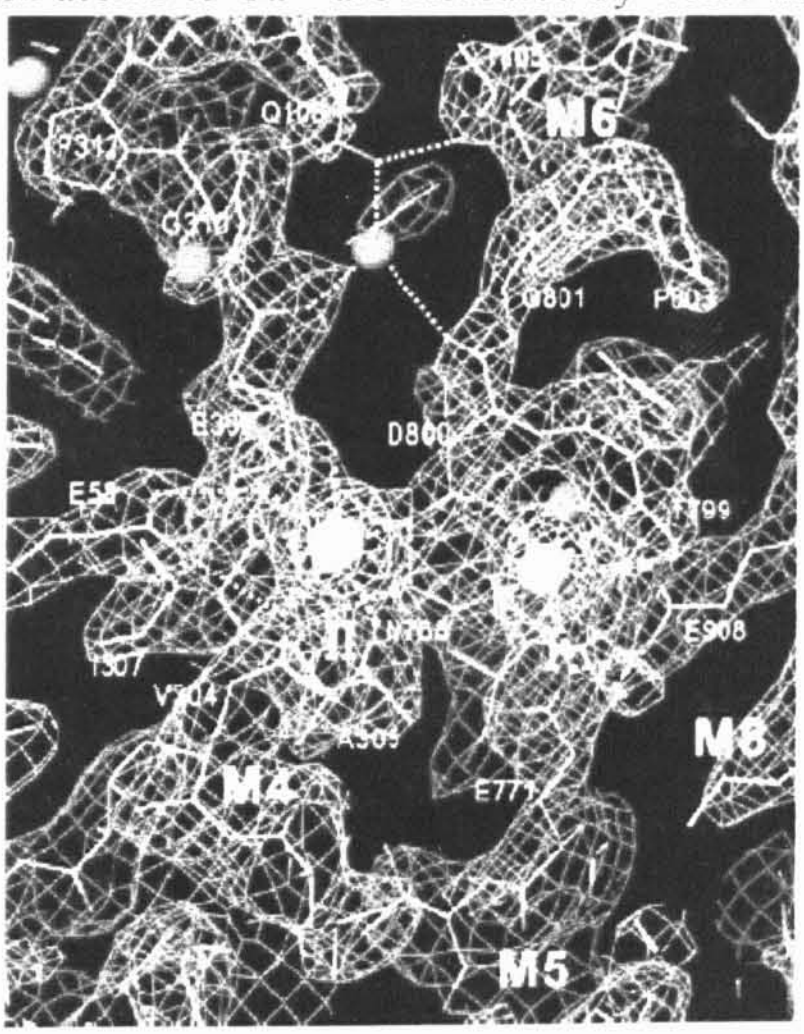

Fig. 5c
Detail of the transmembrane Ca^{2+} binding sites (Toyoshima 2000).
Cyan spheres represent the Ca^{2+} ions and red spheres represent the water molecules. The viewing direction is parallel to the membrane. The coordinations of oxygen atoms to Ca^{2+} are indicated by white dotted lines.

The A-domain probably takes part in the regulation of the Na^+/K^+ ATPase function. This statement is based on the findings of several research groups. Daly (1997) showed that the mutation of Glu^{233} (E233K) dramatically changed the kinetic properties of the rat Na^+/K^+ ATPase. The changes included a higher affinity for ATP and a lower catalytic turnover, which were interpreted as an effect on the E1-E2 conformational equilibrium. Earlier studies on the proteolytic digestion of the renal Na^+/K^+ ATPase also pointed out the regulatory role of the H2-H3 loop and postulated the interaction with the large H4-H5 loop (Lutsenko 1994). Similar effects were thereafter proposed and detected between the A and P domain of SERCA (Toyoshima 2000). It was also proved that the alternations in length and composition of the amino-terminal tail affected the cation specifity and the conformational equilibria (Kaplan 2002).

The P-domain is composed of N- (Leu^{354}-Asn^{377}) and C- termini (Ala^{590}-Leu^{773}) of the H4-H5 loop. The name of this domain suggests the presence of the phosphorylation site, which, indeed, is formed by the Asp^{369} residue that is phosphorylated during the catalytic cycle. As the mutations performed on the P-domain lead often to misfolded protein (Chapman 1998), the studies of this region are rather complicated to perform and the precise mechanism of the phosphorylation is still not completely clarified. Experiments carried out by Patchornik et al. (2000, 2002) using the Fe^{2+} catalysed cleavage of the Na^+/K^+ ATPase predicted the relationship of ATP γ-phosphate, Mg^{2+} and several highly conserved residues in the proximity of Asp^{369} during the phosphorylation process. These predictions are in agreement with the recently published structures of Ca^{2+} ATPase (Sorensen 2004, Toyoshima 2004). As well as in other branches of Na^+/K^+ ATPase research, resolved structures of SERCA will be probably very important for further steps in the exploration of the phosphorylation mechanism.

3.1.1.1 ATP-Binding Site

The N-domain is composed by the central part of the H4-H5 loop, namely Arg^{378}-Arg^{589} and the main region of interest on the N-domain is the ATP binding site. A lot of experiments using a broad range of methods were performed during the last two decades in order to localize amino acid residues involved in the ATP binding. During

the 1984, Farley et al. revealed that the addition of ATP prevents the labelling of Lys^{501} by FITC. This result together with the fact that FITC attached to Lys^{501} cannot be quenched by antifluorescein (Linnertz 1999) led to the conclusion that this amino acid residue is involved in the ATP binding and that it is localized in the depth of the ATP binding site. Using the pyridoxal5'-diphospho-5'-adenosine and pyridoxal phosphate Hinz and Kirley (1990) showed that Lys^{480} is the residue utilized for the recognition of the ATP phosphate moiety. In the 1994, Tran et al. released two subsequent publications on the labelling of Gly^{502} and Lys^{480} by the 2-azido-ATP and 8-azido-ATP meaning also that these residues are likely to be involved in the ATP recognition. The modification of Cys^{549} performed by Linnertz et al. (1998) inhibited the ATP binding as well. Using the point mutations, Scheiner Bobis and Schreiber (1999) confirmed the importance of the Lys^{480} and proposed the significance of Glu^{472} for the activity of the Na^+/K^+ ATPase as well as Teramachi (2002) did for the following residues: Phe^{475}, Lys^{480}, Lys^{501} and Arg^{544}.

In 2000, Toyoshima et al. published the high resolution structure of the Ca^{2+} ATPase, a model of the H4-H5 loop of the Na^+/K^+ ATPase was than computed using the comparative protein modelling method (Ettrich 2001). Several amino acid residues were predicted to be in a close contact with the ATP molecule on the basis of this model and this hypothesis was tested using the S445A, E446Q, F475W (Kubala, 2002) and I417NN422A, R423L, Q482L, E505Q, F548G and F548Y mutants (Kubala 2003a). According to these studies, one of the most important amino acids involved in the ATP binding seems to be the Phe^{475} residue. It probably stabilizes the ATP molecule within the binding pocket through the stacking interaction between its aromatic ring and the adenine ring of the nucleotide (Fig. 6). Another essential residue is the Glu^{446} that forms a hydrogen bond with the NH_2 hydrogen donor of the ATP adenosine moiety. Gln^{482} is not involved in the ATP binding directly. The NH_2 group of this residue stabilizes the sidechain of Glu^{446} by a hydrogen bond over a distance of 2.5Å attracting the glutamic acid closer to the NH_2 group of ATP and thus enabling the Glu^{446}-ATP hydrogen bond formation (Fig. 6). Another indirectly involved residue is the Arg^{423}. Although it resides outside the ATP binding pocket, the Arg^{423} residue can form the hydrogen bond with Glu^{472} over a distance of 1.7Å (Fig. 6). This hydrogen bonding was hypothesized to support the overall shape of the binding pocket and its breaking was thought to result in the complete inability to bind the ATP. Indeed, this hypothesis was recently verified

within the framework of this study (see Chapter 8.3.3.1). Similarly Phe^{548} is not directly involved in the binding of ATP but plays a key role in the supporting the structure and shape of the ATP binding pocket.

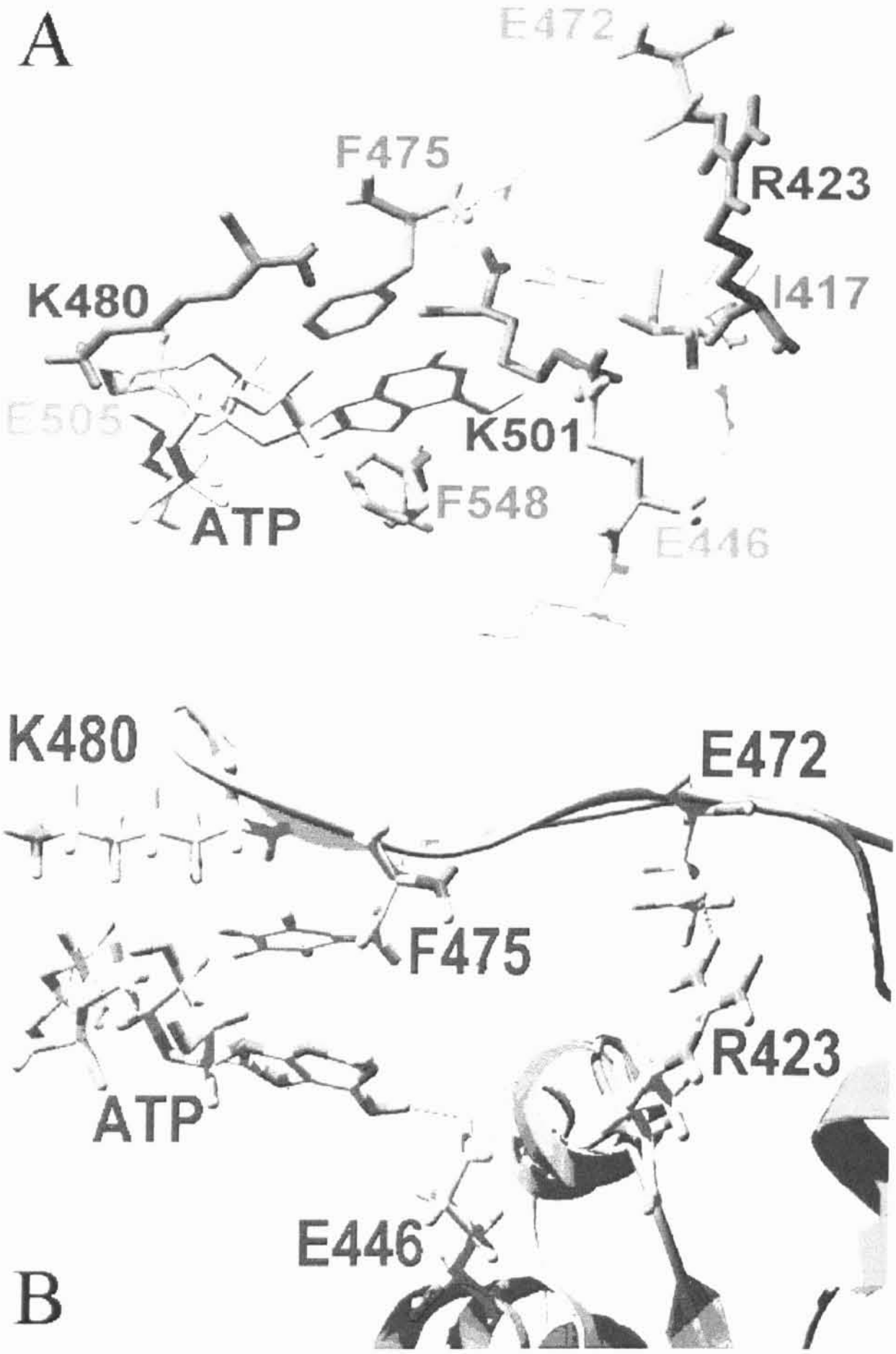

Fig. 6
ATP-binding site of the Na^+/K^+ ATPase (Kubala 2003).
Overall view (panel A) showing some of the key residues for the binding of ATP, and a closer look (panel B) on the hydrogen bonding between Arg^{423} and Glu^{472}, and Glu^{446} and ATP (represented by green dotted lines).

3.1.2. β-subunit

The β-subunit is approximately 55 kDa, membrane protein composed of 370 amino acid residues. It has a single membrane spanning segment, and its amino terminus resides in the cytoplasm. Four isoforms of this protein have been reported. First 30 amino acids are exposed to the cytosol, remaining 300 amino acids form the extracellular part of the β-subunit (Kaplan 2002). There are three N-glycosylation sequences (NXS or NXT) on the extracellular tail and all three are extensively glycosilated. Moreover, three S-S bridges (Kotyk and Amler 1995) can be found in this region (Fig. 7).

Several studies suggested that the β-subunit can be deglycosylated without the loss of its enzymatic activity. Notably, even the substitution of essential asparagine residues prevents glycosylation, but has practically no effect on the catalytic activity (Beggah 1997). In addition, the lack of glycosylation has no effect on the protein delivery to the plasma membrane (Kaplan 2002). These findings are in a great contrast with the closely related β-subunit of the H^+/K^+ ATPase, where the deglycosylation results in the loss of enzyme activity.

Studies using the purified enzyme suggested that both subunits α and β are essential for the enzymatic activity. All experiments using the separated subunits led to the loss of the catalytic activity. In conclusion, β-subunit has probably several roles. Its essential role is in the proper delivery and insertion of the whole enzyme into the plasma membrane (McDonough 1990). Recent studies also revealed that the β-subunit can be directly involved in the mechanism of active transport (Hasler 1998) or in oligomerization of the Na^+/K^+ ATPase (Ivanov 2002). It has been also shown that the reduction of extracellular S-S bridges resulted in the loss of enzymatic activity (Lutsenko 1993). Eakle et al. (1994) found that the changes in the β-subunit can affect the cation affinity of the Na^+/K^+ ATPase.

3.1.3. γ-subunit

γ-subunit is a relatively small peptide with the molecular weight approximately 7 kDa and is a member of the "FXYD" protein family. There are three very similar isoforms of this protein that differ only in several amino terminal residues (Kuster 2000). The γ-peptide is the smallest subunit of the Na^+/K^+ ATPase and is present only when the enzyme is purified from kidneys. Its role is still unclear. Recently, Pu et al. (2002) presented a hypothesis that the γ-subunit may influence and regulate the equilibrium between the main conformational states of the Na^+/K^+ ATPase in an analogy with FXYD regulators that were identified in other tissues.

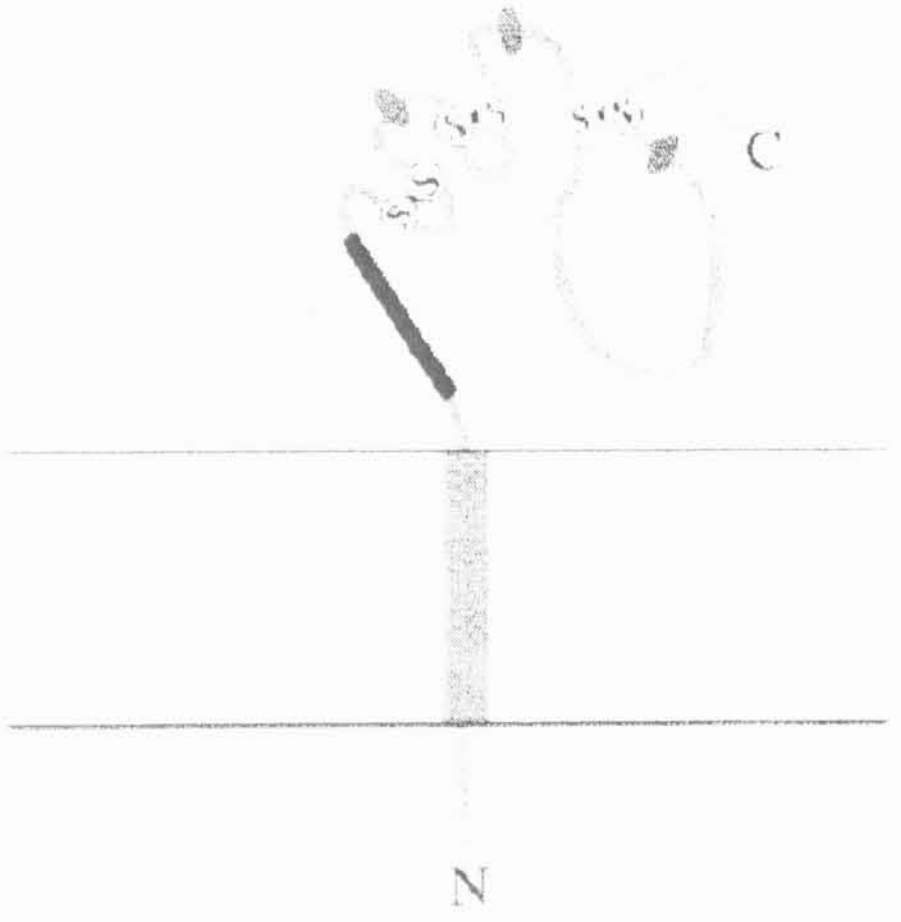

Fig. 7
Outline of the β-subunit. (Kaplan 2002)
The heavy line represents the sequence involved in the association of the β-subunit with the H_7-H_8 loop of the α-subunit. Grey ovals represent the three N-glycosylation sites. S in circles represents the S-S bridges.

3.2. Function - the Catalytic Cycle

The Na^+/K^+ ATPase uses the energy from the ATP hydrolysis to transport actively sodium and potassium ions into and out of the cell. Hydrolysis of one molecule of ATP results in the efflux of three Na^+ and uptake of two K^+ ions. The Na^+/K^+ ATPase affinities for the sodium and potassium molecules are different on the opposite sides of the plasma membrane. On the intracellular side the affinity is high for the sodium (K_d = 0.6mM) and low for potassium (K_d = 10mM). On the extracellular side the affinities are vice versa, low for sodium (K_d = 600mM) and high for potassium (K_d = 0.2mM). The Na^+/K^+ ATPase molecule undergoes two main conformational changes during the catalytic cycle. The main conformations are denoted as E1 and E2 (Jorgensen 1975).

A simple schematic model of the catalytic cycle, known as the Alberts-Post cycle, was proposed (Fig. 8) and recently reinterpreted in terms of the newly published structures of the Ca^{2+} ATPase (Horisberger 2004). Some features of this cycle are still unclear and are subject to a thorough exploration. In particular, the transfer of the phosphate from the ATP binding site to the phosphorylation site, belongs among these puzzles. The A, N and P domains of the α-subunit form the "core engine" of the P-type ATPases. This core engine has the same function in all P-type ATPases and as the sequences of these ATPases are conserved to a substantial extent, it can be expected that the enzymatic mechanism will be similar among all P-type ATPases. An analogy with SERCA will be used to describe this process (Horisberger 2004) in the next paragraph.

Starting in the E1 conformation with the bound ATP molecule (Fig. 8, step 1), three Na^+ ions enter through the open internal gate and bind in their high-affinity binding sites. This induces the following conformational change. First, the N-domain undergoes a large rotational movement that positions the γ-phosphate of ATP close to the phosphorylation site. In this position ATP becomes a sort of crosslinker between the N- and P-domains and can be thereafter cleaved allowing the phosphorylation of the D376 residue (step 2). Second, the A domain rotates by ~30° around a horizontal axes (Toyoshima 2004), producing the large translation of the first transmembrane segment toward the intracellular side and a 90° kink in the internal third of this helix. According to Toyoshima (2004) and Sorensen (2004), this movement of the helix is responsible for the closing of the internal gate (step 3). This step is also accompanied by the release of the ADP and results in the E1-P state. This high energy E1-P state relaxes rapidly to the

E2-P conformation with opening of the extracellular gate (step 4) accompanied with the change of the cation affinity and release of the Na^+ ions to the

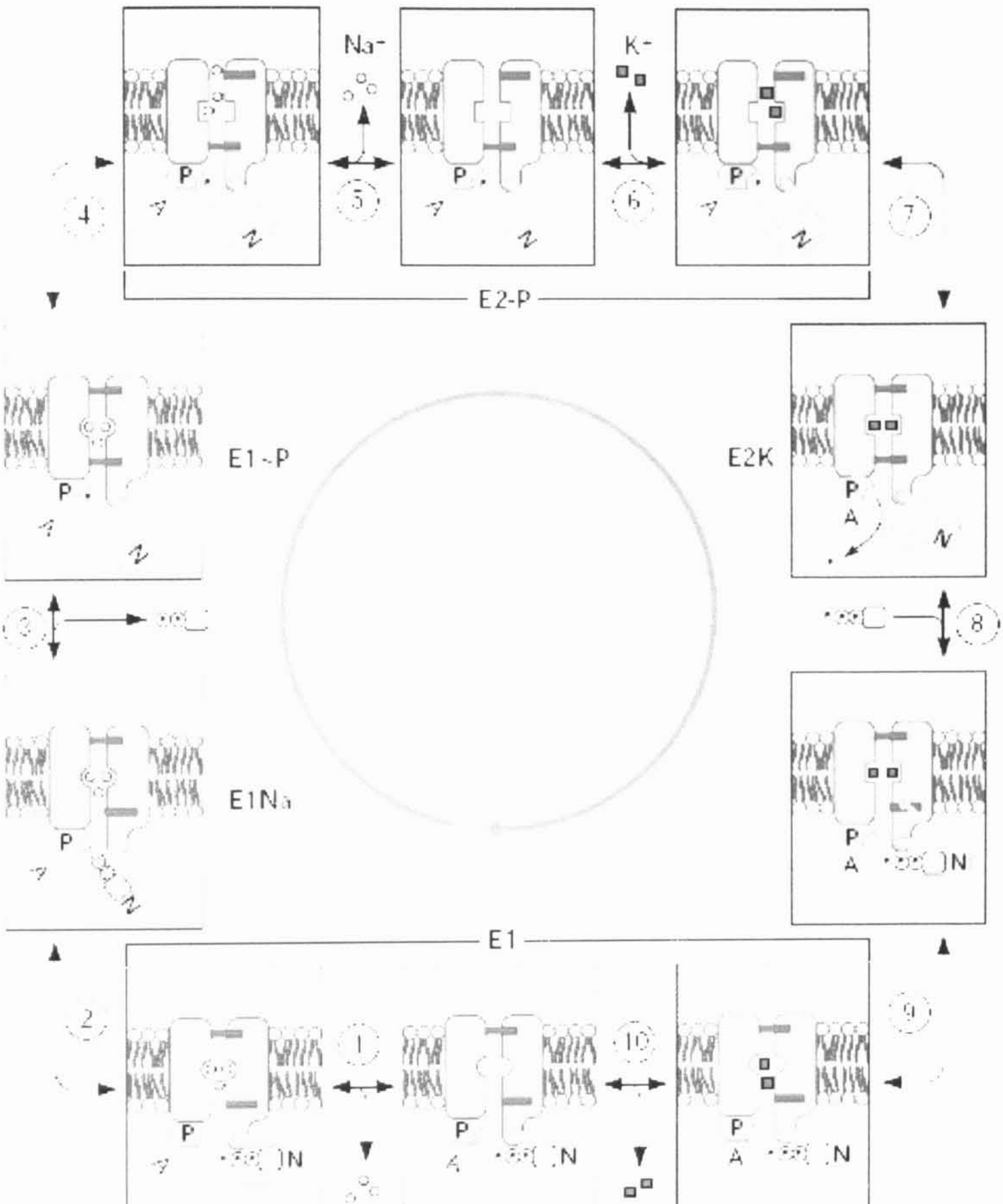

Fig. 8
Catalytic cycle of the Na^+/K^+ ATPase. (Horisberger 2004)
The steps are described in text. Circular arrow shows the direction of the physiological cycle driven by the high ATP/ADP ratio. However, all of the steps are reversible and under appropriate circumstances, the cycle can run in the reverse direction.

extracellular space (step 5). The enzyme is now ready for the uptake of two extracellular K^+ ions (step 6). Binding of these results in two major changes, the dephosphorylation of D376 and the occlusion of the K^+ ions by the closure of the extracellular gate (step

7). The N-domain is now accessible to the intracellular nucleotide, which binds to the ATP-binding site (step 8). This promotes the conformational change from the E2K to the E1 conformation which includes the opening of the intracellular gate (step 9) and the release of K^+ ions to the intracellular space (step 10). Notably, these steps may also occur in the absence of the nucleotide but at a much lower rate (Horisberger 2004). The catalytic cycle is also a reversible process, the Na^+/K^+ ATPase can thus, under specific conditions, synthesize ATP (Garrahan 1967).

Although the description of the catalytic cycle summarized in previous paragraph is based on the similarity to the Ca^{2+} ATPase and is in accordance with the majority of the experimental work, some results exist that cannot be thus explained (for details see Askari 1982). Several alternative models were, hence, suggested. The idea of several ATP binding sites per molecule (Ward 1996) was rejected during the years by many authors, however the possibility that Na^+/K^+ ATPase works as a dimer (Repke 1973) or even a tetramer (Taniguchi 2001) was not still either proved or declined. The idea of an oligomeric character of the Na^+/K^+ ATPase was also supported recently by the finding that the α-subunit (Donnet 2001) as well as the β-subunit (Ivanov 2002) can form oligomers.

4. Research Strategy - Molecular Modelling, Protein Mutagenesis and Fluorescence Spectroscopy

In order to obtain structural information about the H4-H5 loop of the α-subunit of the Na^+/K^+ ATPase, two research methods were employed simultaneously. First, it is a theoretic prediction of the structure using the restraint based homology modelling. Second, it is the protein mutagenesis and expression and consequent examination of the mutated proteins by the means of the fluorescence spectroscopy. These two branches of our research ran more or less independently, and the results of both, the modelling and spectroscopic part, were then confronted (Kubala 2004a).

In this work, we were mainly interested in the characterisation of the ATP-binding site of the Na^+/K^+ ATPase. For this part, several amino acid residues possibly involved in the ATP binding were selected, mutated and the ATP binding to these mutants was subsequently analysed. The number and position of the TNP-ATP binding sites was another question. In order to investigate this part, another set of point mutants and several truncated H4-H5 loops were proposed, constructed and the ligand binding was analyzed. Finally, we were interested also in the structural stability of the large cytoplasmatic H4-H5 loop of the Na^+/K^+ ATPase, which was inspected by the fluorescence anisotropy measurements.

The first step was the construction of a molecular model of the H4-H5 loop. This model was originally made in an analogy with the Ca^{2+} ATPase from the endoplasmatic reticulum (Ettrich 2001), that was crystallized at 2.6Å resolution (Toyoshima 2000). Recently, the crystal structure of the N-domain of the Na^+/K^+ ATPase (Hakanson 2003) appeared. However, this structure lacks three segments, so we had to combine both mentioned crystal structures to obtain the best possible model of the H4-H5 loop, as described in the Molecular Modelling section. All point mutants and truncated loops used in this study as well as the interpretation of all results were based on this model.

Second step was the construction of the mutated proteins and truncated loops. The DNA coding the H4-H5 loop was ligated into the pGEX vector, containing the gene for the ampiciline resistance and sequence coding the GST, so that our constructs were expressed as a GST-H4-H5 loop fusion proteins. The expression of the proteins was performed in *E. coli* bacteria using the pGEX expression vector. The purification of the

enzymes was carried out using the standard procedures of the affinity chromatography, the GST part of the fusion protein was bound specifically to the glutathione-Sepharose column and the fusion protein was subsequently eluted by the reduced glutathione. The presence of the GST in the fusion protein didn't affect the results in the binding experiments due to the lack of ATP binding site. For the fluorescence anisotropy studies, the GST fusion protein was cleaved by thrombin and the GST was thereafter removed by the incubation with the glutathione-Sepharose column. For detailed description of these procedures, see the Molecular Biology section.

The final part of our study was the analysis of the ATP binding, and the investigation of the structural stability of the H4-H5 loop using the expressed and purified protein constructs.

The ATP binding was explored using the TNP-ATP, the ATP-fluorescent analog. This fluorescent dye is sensitive to the polarity of its environment, so that the probe binding can be monitored by the increased intensity of fluorescence. The protein sample was titrated by the aliquots of TNP-ATP, the intensity of fluorescence was recorded and fitted to the theoretical curve (Kubala 2003). In this way, the dissociation constant for TNP-ATP was assessed. Using this dissociation constant, the dissociation constant for ATP was determined by the competition of the TNP-ATP and the ATP for the ATP-binding site. The competition experiments were carried out in an analogy to the TNP-ATP binding experiments. The protein sample containing the ATP was titrated by the TNP-ATP, the experimental points were fitted to the theoretical dependence (Kubala 2004) and the dissociation constant for ATP was extracted. The ATP dissociation constant for a point mutant lacking some particular amino acid residue was compared to the wild-type dissociation constant and the influence of this amino acid residue on the ATP binding was interpreted using the molecular model (Lansky 2004). The FITC fluorescence anisotropy measurements as well as the eosin steady state fluorescence measurements were performed to investigate the rigidity of the N-domain of the Na^+/K^+ ATPase. For details, see the Fluorescence Spectroscopy and the Results and Discussion sections.

5. Molecular Modelling

5.1. Homologous Crystal Structure - Ca^{2+} ATPase

The main object of our study was the structure of the Na^+/K^+ ATPase, however, we have also to mention the main characteristics of the Ca^{2+} ATPase from sarco(endo)plasmatic reticulum (SERCA), (Fig. 9), since it is one of the most intensively studied homologous proteins to the sodium pump, which provides a significant source of relevant information to the Na^+/K^+ ATPase research. The Ca^{2+} ATPase, which belongs to the Type IIA family of the P-type ATPases (Axelsen 1998), is involved in the skeletal muscle relaxation through the transport of Ca^{2+} ions across the membrane of sarcoplasmatic reticulum. This integral membrane protein of molecular weight 110 kDa and containing approximately 1000 amino acid residues (MacLennan 1985) can transport 2 Ca^{2+} from the cytoplasm to the lumen of sarcoplasmatic reticulum against the concentration gradient, in exchange for 2 or 3 H^+ per ATP hydrolysed (Toyoshima 2004). In muscle cells, the Ca^{2+} ions are stored in sarcoplasmatic reticulum and are released to the cytosol for contraction and the Ca^{2+} ATPase is responsible for pumping the Ca^{2+} ions back to sarcoplasmatic reticulum causing the muscle relaxation.

Recently, high resolution structures of SERCA in several conformations were determined using the X-ray crystallography. The most important are the two main conformations: Ca^{2+}-bound E1 state, solved at 2.6Å resolution (PDB accession code 1EUL) (Toyoshima 2000), and Ca^{2+}-unbound E2 state stabilized with thapsigargin, solved at 3.1Å resolution (PDB accession code 1IWO) (Toyoshima 2002). In addition to these, the enzyme was also crystallized with other bound ligands, as for example ATP analog or Mg^{2+} (Toyoshima 2004, 2004a). Several publications followed these fundamental results and analyzed the implications of the structural changes on the catalytic cycle and transport mechanism of SERCA (reviewed in Toyoshima 2004a).

These findings had also a great impact on the Na^+/K^+ ATPase research. After the publication of the E1 conformation of SERCA, the model of the H4-H5 loop could be computed according to the Ca^{2+} ATPase crystal structure (Ettrich 2001). This model had an essential impact on further experiments (Kubala 2002, 2003a, Hofbauerova 2002, 2003) and is used for the interpretation of the experimental results up to now with just

several improvements. During 2004, the N-domain was newly remodelled according to the crystal structure of the N-domain of the porcine Na^+/K^+ ATPase (Hakkanson 2003, Haue 2003),

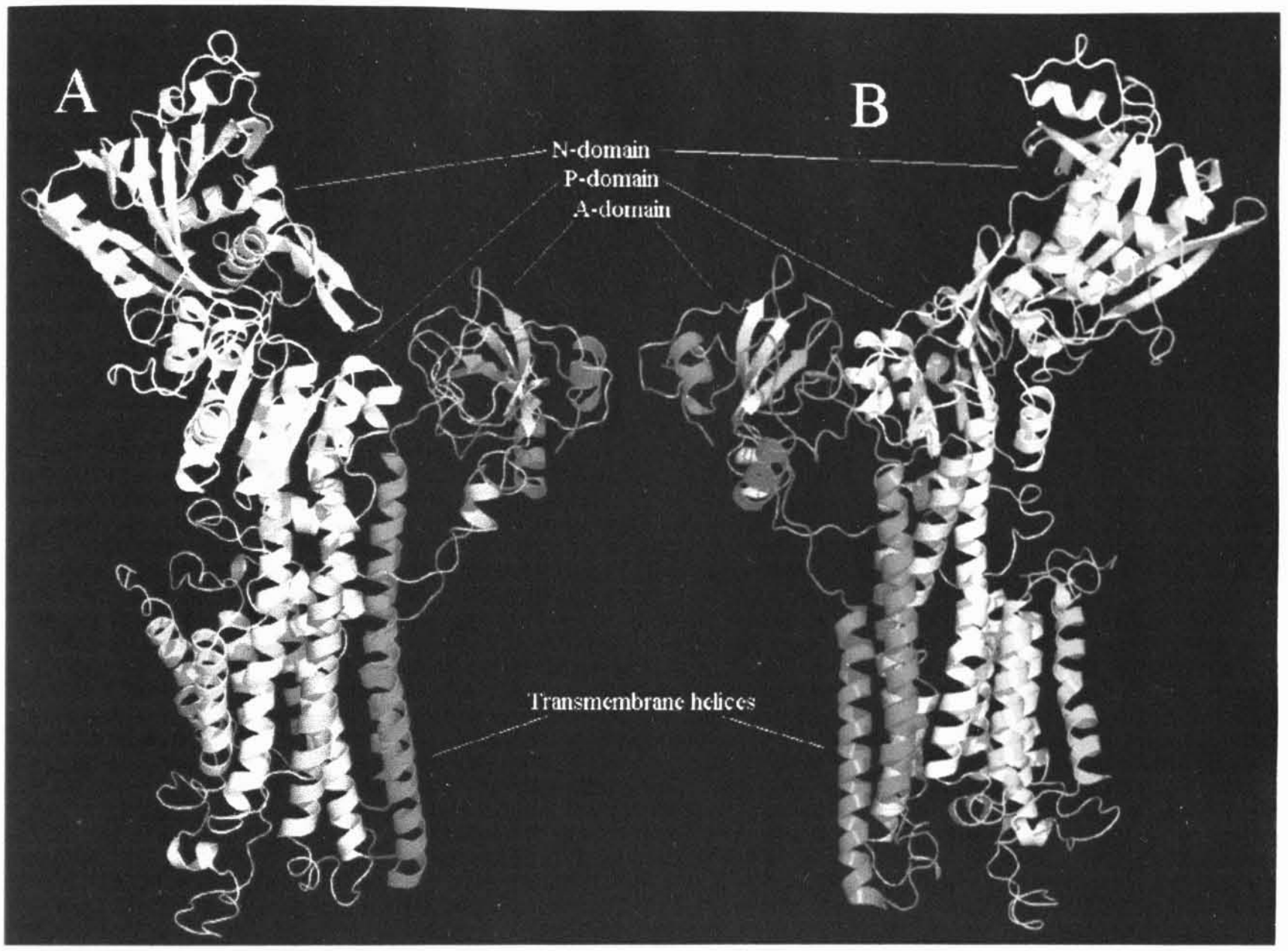

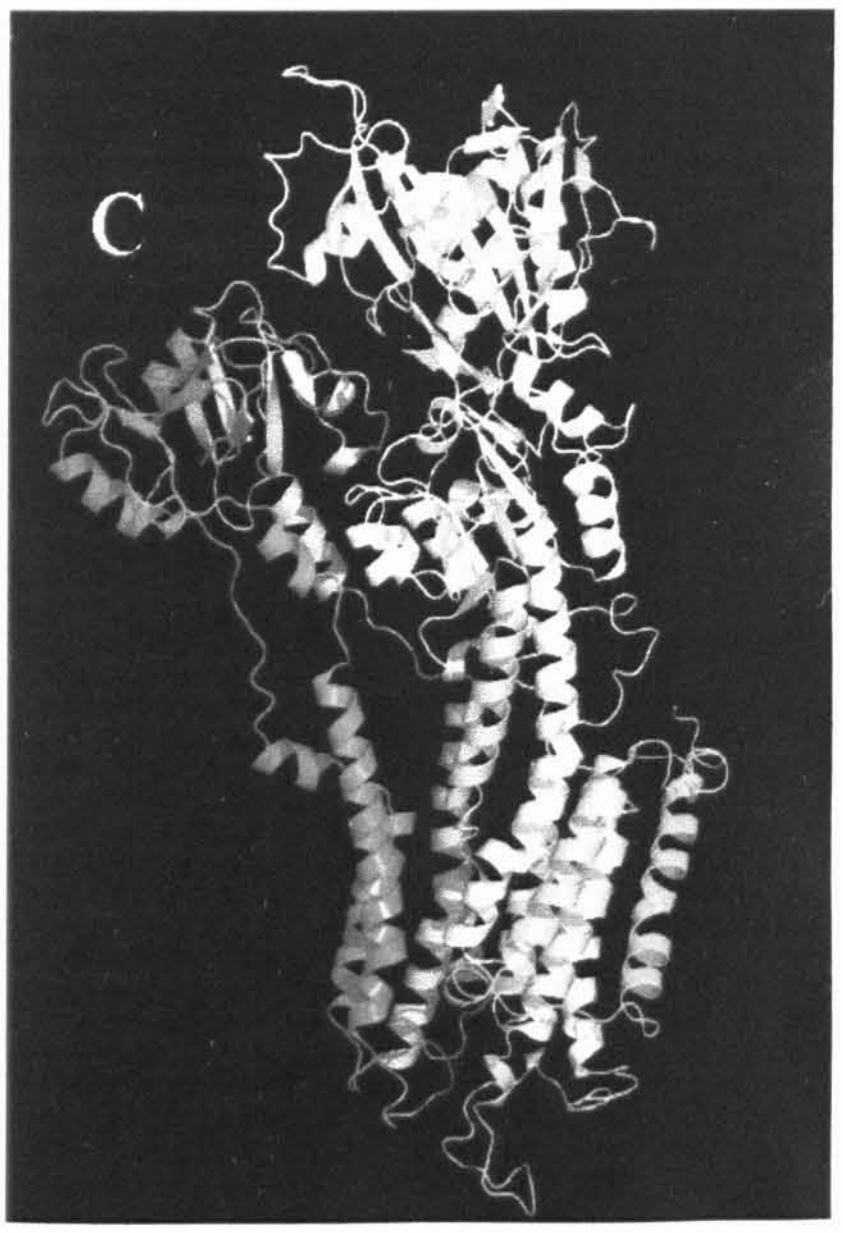

Fig. 9
Crystal structure of the Ca^{2+} ATPase.
Panels (A) and (B) depict the E1 conformation (PDB code 1EUL, Toyoshima 2000) of the calcium pump from opposite directions. Color changes gradually from the N-terminus (blue) to the C-terminus (red). E2 conformation (PDB code 1IWO, Toyoshima 2002) depicted in the same color coding is on the panel (C). Note the large movement of the N- and A-domains towards the P-domain.

which lacked three 6, 10 and 6 amino acid residue long loops important for the nucleotide binding.

Similarly, the enzymatic cycle of the Na^+/K^+ ATPase is recently interpreted in terms of the Ca^{2+} ATPase crystal structures (Horisberger 2004). One of the greatest mysteries of the catalytic cycle of the Na^+/K^+ ATPase had been for a long time the process of phosphorylation, because the ATP binding site and the phosphorylation site are approximately 30Å apart. The recent crystal structures of SERCA provide a completely new view on this issue. Like for SERCA, it has been suggested that the N-domain moves upon the ATP binding towards the P-domain, with the ATP forming a sort of "crosslinker" between them (Horisberger 2004). This large movement brings the γ-phosphate near the phosphorylation site. Together with the movement of A-domain it subsequently leads also to the closing of the internal gate and occlusion of Na^+ ions. A computation of this large mutual movement of the N- and P-domain is currently in progress in order to verify this hypothesis suggested by the Ca^{2+} ATPase analogy. Several nanoseconds of the life of the H4-H5 loop will be simulated using the molecular dynamics and the results will be compared to the crystal structures of SERCA in different conformations.

5.2. Restraint Based Homology Modelling

Two methods are usually employed for the investigation of the 3D-structure of proteins; the X-ray crystallography and NMR spectroscopy. These methods are very sophisticated and require highly purified protein sample in relatively big quantities. Moreover, the probability of obtaining a satisfactory result is rather low in the case of a large protein.

Restraint based homology modelling, which is relatively quick and straightforward, is a great tool of protein structure analysis in cases when the protein expression level is relatively low or the protein is too large. The only condition that allows the usage of this method is an existence of the template; a homological molecule. A detailed description of the procedure of the restraint based homology modelling is beyond the scope of this work. Therefore a rough outline will only be mentioned. For more information, see the description and manuals of the software used in this study:

http://www.es.embnet.org/Doc/clustalw/clustalx.html,

http://salilab.org/modeller/,

http://www.scripps.edu/mb/olson/doc/autodock/,

http://www.biochem.ucl.ac.uk/~roman/procheck/procheck.html,

http://www.accelrys.com/products/insight/.

The homology modelling of proteins consists of three major steps, the alignment of the primary sequences of the known 3D-structure and the desired protein (Fig. 10), the computation of the model itself and the refinement of the computed model. The model has to be checked afterwards by a specialised software and additional features, as for example ligand docking, can be computed.

We used the Ca^{2+}-ATPase from the sarcoplasmatic reticulum as the original template protein. This protein shows 32.8% identity and 53.3% similarity to the Na^+/K^+-ATPase and its tertiary structure has been solved at 2.6Å resolution by the X-ray crystallography (Toyoshima 2000). Another, newer, template was the crystal structure of the N-domain of the porcine Na^+/K^+-ATPase solved also at 2.6Å resolution (Hakanson 2003), which however lacks three 6, 10 and 6 amino acid residue long loops at the crucial regions of the protein. The first model of the H4-H5 loop of the Na^+/K^+-ATPase, made by Ettrich et al. in 2001, was based on the Toyoshima's SERCA crystal

structure. After Hakanson's publication, our model was refined according to this new structure (Fig. 11).

```
Mouse-brain     RMTVAHMWFDNQIHEADTTENQSGVSFDKTSATWFALSRIAGLCNRAVFQANQENLPILK 437
Crystal         MMTVAHMWFDNQIHEADTT------TFDKRSPTWTALSRIAGLCNRAVF----------K
peptid1         --------------------ENQSGV-------------------------------------
peptid2         ---------------------------------------------------QANQFNLPII-
peptid3         ------------------------------------------------------------
                 ******************       *** * ** **************          *

Mouse-brain     RAVAGDASESALLKCIEVCCGSVMEMREKYTKIVEIPFNSTNKYQLSIHKNPNASEPKHL 497
Crystal         RDTAGDASESALLKCIELSCGSVRKMRDRNPKVAEIS------YQLSIHEREDNPQS-HV
peptid1         ------------------------------------------------------------
peptid2         ------------------------------------------------------------
peptid3         ---------------------------------------FNSTNK----------------
                *   *************  ****  **    *  **       ******          *

Mouse-brain     LVMKGAPERILDRCSSILLHGKEQPLDEELKDAFQNAYLELGGLGERVLGFCHLLLPDEQ 557
Crystal         LVMKGAPERILDRCSSILVQGKEIPLDKEMQDAFQNAYLELGGLGERVLGFCQLNLPSGK
                ******************  *** *** *  ********************** * **

Mouse-brain     FPEGFQFDTDEVNFPVDNLCFVGLISMID 586
Crystal         FPRGFKFDTDELNFPTEKLCFVGLMSMID
                ** ** ***** ***   ****** ****
```

Fig. 10
Sequence alignment of the N-domain of the α_1-subunit of mouse brain Na^+/K^+-ATPase with that of the porcine α_2-subunit of Na^+/K^+-ATPase, whose tertiary structure has been solved recently at 2.6 Å resolution by X-ray crystallography and for which the PDB coordinates are available. Three 6, 10, and 6 residue long peptides from our published structure of the complete pig-kidney Na^+/K^+-ATPase were aligned to fill the gaps in the recently published structure. Identical amino acids are marked by an asterisk.

The primary structure of the mouse brain Na^+/K^+ ATPase from Arg^{378} to Asp^{586} was aligned with the template sequences by CLUSTALX (Thompson 1997). The sequence alignment used for the modelling is shown in Figure 10. The three-dimensional model constituted by all non-hydrogen atoms was built and examined by the MODELLER6 package (Sali 1993). The tertiary structure model was checked with PROCHECK (Laskowski 1993).

The crystal structure of TNP-ATP was extracted from the PDB coordinates file, 1D1Q (Wang 2000). These were deposited in the Protein Data Bank (http://www.pdb.org). Hydrogens were added using the BIOPOLYMER module included in INSIGHT II (Accelrys Inc., San Diego, CA, USA). The point charges of the TNP-ATP were thereafter calculated using Gaussian98 package (Lansky 2004). Docking of ATP and TNP-ATP was explored with AUTODOCK (Morris 1996). To complete the modelling of the truncated peptides, energy minimization was performed

using the parameters and methods published for pig kidney Na^+/K^+ ATPase (Ettrich 2001). Several molecular dynamics runs were set up for a canonical ensemble. One molecular dynamics run was a single interval of 120 ps at 300 K, and 343 K, respectively, with a femtosecond time step, result being recorded every 25 fs. The shake technique was applied to all bonds. Force field parameters were the same as for the minimization. FITC was connected to K501 via a covalent bond using the BUILDER module included in INSIGHT II and its position in the binding site was optimized.

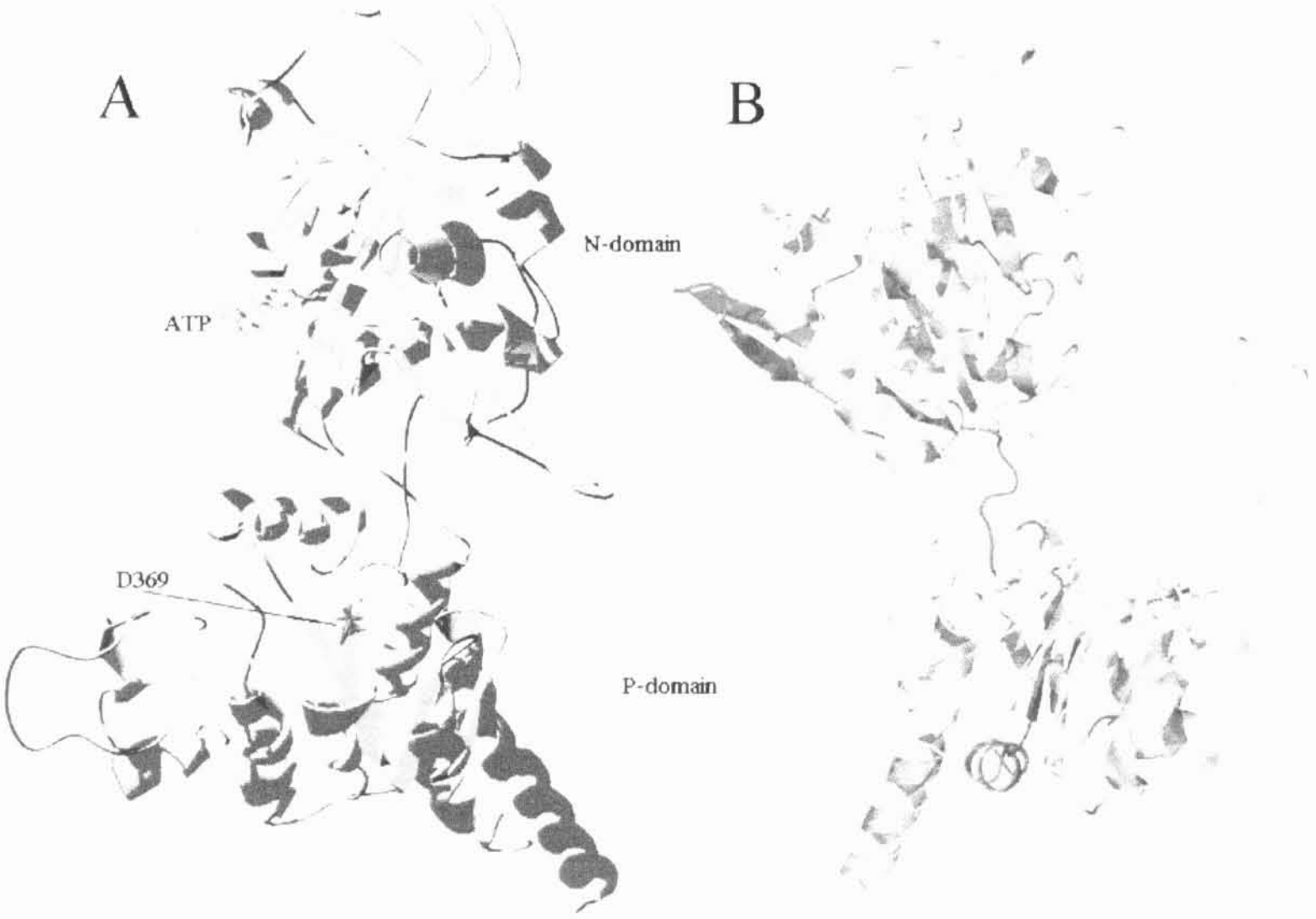

Fig. 11
Model of the H4-H5 loop constructed in the analogy with the SERCA crystallographic structure (Toyoshima 2000) and the structure of N-domain of the Na^+/K^+ ATPase. Two different color representations: (A) α-helices are depicted in red, β-sheets in yellow and the phosphorylation site (D369) in blue. (B) Colour changes gradually from the N-terminus (blue) to the C-terminus (red).

6. Molecular Biology

6.1. Site Directed Mutagenesis

Proteins with the Leu^{354}-Ile^{604} sequence denoted also as wild-type (WT) or K605 and all point mutants were produced by the following process. The H4-H5 (Leu^{354}-Ile^{777}) sequence was obtained by polymerase chain reaction (PCR) using α-subunit of the mouse brain Na^+/K^+ ATPase as a template. The DNA sequence was amplified by the PCR in the presence of PCR primer pairs for the desired sequence and subsequently purified on an agarose gel. This DNA sequence was thereafter subcloned to the pGEX-2T expression vector using the *Bam*HI and *Eco*RI restriction enzymes; the stop-codon was inserted on the position 605. The pGEX-2T plasmid contains the gene for the GST and the gene causing the ampiciline resistance (Fig. 12) (Obsil 1998).

The wild type DNA sequence was used for further point mutations. These mutations were performed by the PCR using the QuickChange Kit (Stratagene). The PCR procedure is as follows:

1. Denaturation of the plasmid at 95 °C for 60 s.
2. Denaturation of the plasmid at 95 °C for 30 s (upstream and downstream strands of the circular double-stranded DNA are separated).
3. Annealing of primers at 51 °C for 60 s (the decrease in the temperature allows the primers to attach the circular single strands of denatured DNA).
4. Extension at 68 °C for 9 min (DNA polymerase synthesizes the reverse complement to each strand of DNA; this temperature is optimal for the synthesis by PfuUltra™ HF DNA polymerase).

Steps 2-4 are repeated 20 times, each cycle results in duplication of DNA molecules.

5. The mixture is incubated for additional 10 min at 68 °C.
6. The nonmutated, methylated parental DNA is digested with 1 μl of the restriction enzyme DpnI (10U/μl) for 1 h at 37 °C.

And the PCR reaction mixture was:

40 µl distilled water

5 µl 10x PfuUltra™ HF reaction buffer (Stratagene)

1 µl 10 mM dNTP

1 µl template DNA (50-100 ng)

1 µl the upstream primer (100 pmol/µl)

1 µl the downstream primer (100 pmol/µl)

1 µl PfuUltra™ HF DNA polymerase (2.5 U/µl)

The PfuUltra™ HF reaction buffer consists of 100 mM KCl, 100 mM $(NH_4)_2SO_4$, 200 mM Tris-HCl (pH 8.8), 20 mM $MgSO_4$, 1% Triton® X-100 and 1 mg/ml nuclease-free bovine serum albumin (BSA).

The point mutations were introduced into the wild-type sequence using the PCR primers (step 3) with altered nucleotides. The upstream primers for performed mutations were (nucleotides in bold and underlined font encode the mutated amino acid):

D443A: 5'-CTT AAG CGT GCA GTA GCG GGA G**C**T GCT TCC GAG TCG GCG-3',

E472A: 5'-G TAC ACC AAG ATA GTG **T**AG ATT CCT TTC AAC TCC ACC-3',

S477A: 5'-GTG GAG ATT CCT TTC AAC **G**CC ACC AAC AAG TAC CAG CTC TCC-3',

P489A: 5'-CAG CTC TCC ATT CAC AAG AAC **G**CA AAC GCA TCG GAG CC-3',

M500A: 5'-CCT AAG CAC CTG CTA GTG **GC**G AAG GGC GCC CCA GAA AGG-3',

R423LE472A: 5'-GA ATT GCT GGT CTC TGT AAC **CT**G GCA GTG TTT CAG GCT AAC C-3' and primer for mutation E472A (used subsequently).

N398D: 5'-GCT GAC ACC ACA GAG **GAT** CAG AGT GGG GTC TCC-3'

D369A: 5'-CCA CCA TCT GCT CC**G CC**A AGA CTG GAA CTC TGA C-3'

The downstream primers were reverse complementary.

Loops of different lengths were produced from the H4-H5 (Leu^{354}-Ile^{777}) sequence by the insertion of stop codons into the sequence at the positions of K605, R589, C577, G542 and K528, respectively. The N-terminal shortened construct I390–S601 was made by subcloning the corresponding DNA sequence into the multiple cloning site of an empty pGEX-2T vector between *Bam*HI and *Eco*RI sites as described above. The following primers were used for the amplification of different constructs, with the relevant site in bold and underlined font in each case:

L354–I777 sense with *Bgl*II site: 5'-CGT **AGA TCT** CTG GAA GCT GTG GAG ACC-3';

antisense with *Eco*RI site: 5'-AT**G AAT TC**C AAT GTT ACT TGT TAG GGT-3';

L354–I604 sense with stop codon: 5'-C AGC GCT GGG ATT **TAG** GTC ATC ATG GTC-3';

antisense with stop codon: 5'-C TCC TGT GAC CAT GAT GAC **CTA** AAT CCC AGC-3';

I390–S601 sense with *Bgl*II site: 5'-G CGT **AGA TCT** ATC CAT GAA GCT GAC ACC ACA G-3';

antisense with *Eco*RI site: 5'-AT **GAA TTC** GCG CTG CGG CAT TTG CCC ACA GC-3';

L354–P588* sense with stop codon: 5'-ATT GAC CCT CCT **TGA** GCT GCT GTC CCC GAT GCT GTG-3';

L354–L576* sense with stop codon: 5'-CCC GTG GAT AAC CTC **TGA** TTC GTG GGT CTT ATC TCC-3';

L354–L541* sense with stop codon: 5'-GGC CTT GGA **TAG** CGT GTG CTA GGT TTC TGC CAC CTC-3';

L354–L527* sense with stop codon: 5'- CCC CTG GAC GAA GAG CTG **TAA** GAC GCC TTT CAG AAT GCC-3';

the * symbol means that antisense primers of the C-terminally shortened constructs were usually complementary.

The DNA sequence containing the point mutation or shortened loop was transformed into the *E. coli* XL1-Blue supercompetent cells using the heat shock method. This

method is based on a temporal disruption of the cell membrane integrity using several sudden changes of temperature allowing a penetration of the DNA into the cytosol. The heat shock sequence was:

1. The cells were incubated with the plasmid on ice for 30 min.
2. The mixture was inserted in a bath of 42 °C for 45 s.
3. The mixture was placed on ice for 2 min.
4. 200 µl of LB medium (10 g bacto-tryptone, 5 g bacto-yeast extract and 10 g NaCl in 1 liter of distilled water, pH adjusted to 7.4 by NaOH) warmed to 42 °C was added and the suspension was incubated at 37 °C for 1 h.

The cells were grown overnight at 37 °C on the agar plates containing the LB medium with ampicilin (50 µg/ml) in order to suppress the non-transformed cells. Single colony was chosen and cultivated overnight in 3 ml of liquid LB medium containing ampicilin (50 µg/ml) at 37 °C. The cells were thereafter disrupted and the DNA was harvested and purified using QIAprep Spin Miniprep Kit (Qiagene). DNA was eluted into 50 µl of TE buffer (10 mM Tris-HCl, 1 mM EDTA, pH 8.0) and stored in -20°C. Sequence of the mutated DNA was determined by ABI Prism automated sequencer.

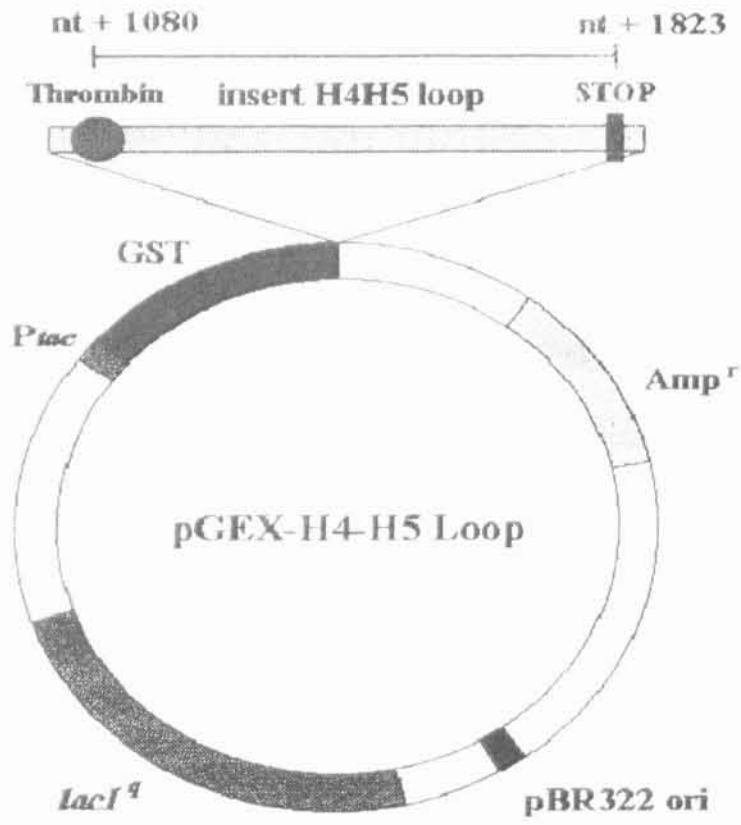

Fig. 12
A sketch of the expression vector pGEX-2T containing the H4-H5 loop insert. The pGEX-2T vector contains the gene coding the GST and the gene causing the ampicillin resistance. GST protein can be removed by the cleavage of the fusion protein using thrombin, the cleavage site is represented by a black circle.

6.2. Protein Expression and Purification

Mutated DNA (pGEX-2T plasmid containing the DNA coding for a point-mutated H4-H5 loop) was transformed into *E. coli* BL21 cells using the heat-shock method, as described above. Cells were grown overnight on agar plates containing the LB medium with ampicilin (50 μg/ml) in order to suppress the non-transformed cells. Single colony was chosen and cultivated overnight in 3 ml of liquid LB medium containing ampicilin (50 μg/ml). This suspension was diluted into 250 ml of liquid LB medium containing ampicilin (50 μg/ml) and cultivated to O.D. 0.8 at 600 nm. Up to this point the temperature was 37 °C for all cultivations. IPTG, that induces the expression of the GST-fusion protein, was than added (final concentration 0.1 mM) and the cells were cultivated overnight at 30 °C.

Suspension was centrifuged at 4 °C and 5000 g for 30 minutes and the pellet, containing the *E. coli* bacteria was collected. It was resuspended in TENG buffer (50 mM Tris-HCl, pH 7.5; 1 mM EDTA; 100 mM NaCl; 10% glycerol; 1% NP-40; 1 mM DTT) containing the protease inhibitors (1 mM PMSF, 2 μg/ml leupeptin, 2 μg/ml pepstatin, 20 μg/ml aprotinin) and incubated with lysozyme (0.5 μg/ml) for 15 minutes on ice. Cells were disrupted by sonication. Cell debris was centrifuged at 4 °C and 15000 g for 30 minutes and the supernatant was loaded into the 2 ml glutathione-Sepharose 4B column (equilibrated with TENG buffer). It was incubated for 1.5 hour and washed by 200 ml of buffer (20 mM Tris-HCl pH 7.4; 140 mM NaCl). The GST-fusion protein was eluted by threefold addition of 2 ml 50 mM Tris-HCl, pH 8, containing 10 mM reduced glutathione (Smith and Johnson 1988, Ennis 1997) and dialyzed overnight at 4 °C against the 1000-fold excess of 50mM Tris-HCl, pH 7.5 and stored at -20 °C.

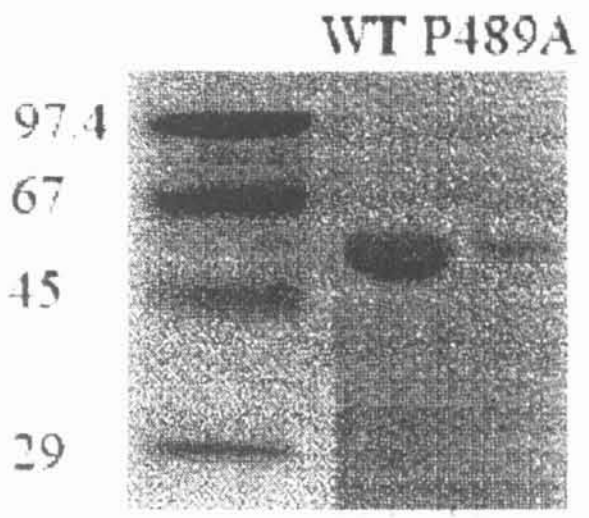

Fig. 13
SDS-PAGE: Expression and purification of GST fusion proteins. The expression level for the P489A mutant was lower than that for the wild type. All other mutants were expressed comparably to the wild type.

Protein purity was determined by the 12 % (w/v) SDS-PAGE process. Single band corresponding to approximately 53 kDa was detected on the electrophoresis gel. All mutants had the expression level similar to the WT, except for the P489A mutant, that was expressed significantly less (Fig. 13). Concentration was estimated by the Bradford method (Bradford 1976) using 1mg/ml BSA as a standard.

7. Fluorescence Spectroscopy

7.1. ATP Binding Measurements

ATP binding to the H4-H5 loop - GST fusion proteins was measured indirectly using 2',3'-O-(2,4,6-trinitrophenyl) adenosine 5'-triphosphate (TNP-ATP) (Fig. 14), a fluorescent analog of ATP.

Quantum yield of TNP-ATP is sensitive to the polarity of its environment (Hiratsuka 1973, 1973a). Therefore, the binding of the probe to the protein could be detected by the changes in fluorescence intensity. The increase of the fluorescence intensity accompanied by a blue shift is observed upon the binding of the probe (Fig. 15). Binding of the TNP-ATP was characterized by the titration of a protein sample by the fluorescent probe and evaluation of the dissociation constant. A method of data analysis employing the nonlinear least square fitting procedure (Kubala 2003) was used in our computations instead of classical Scatchard-plot approach (Moczydlowski and Fortes 1981a), which artificially shifts the estimated value of dissociation constant as demonstrated by Kubala et al. (2003).

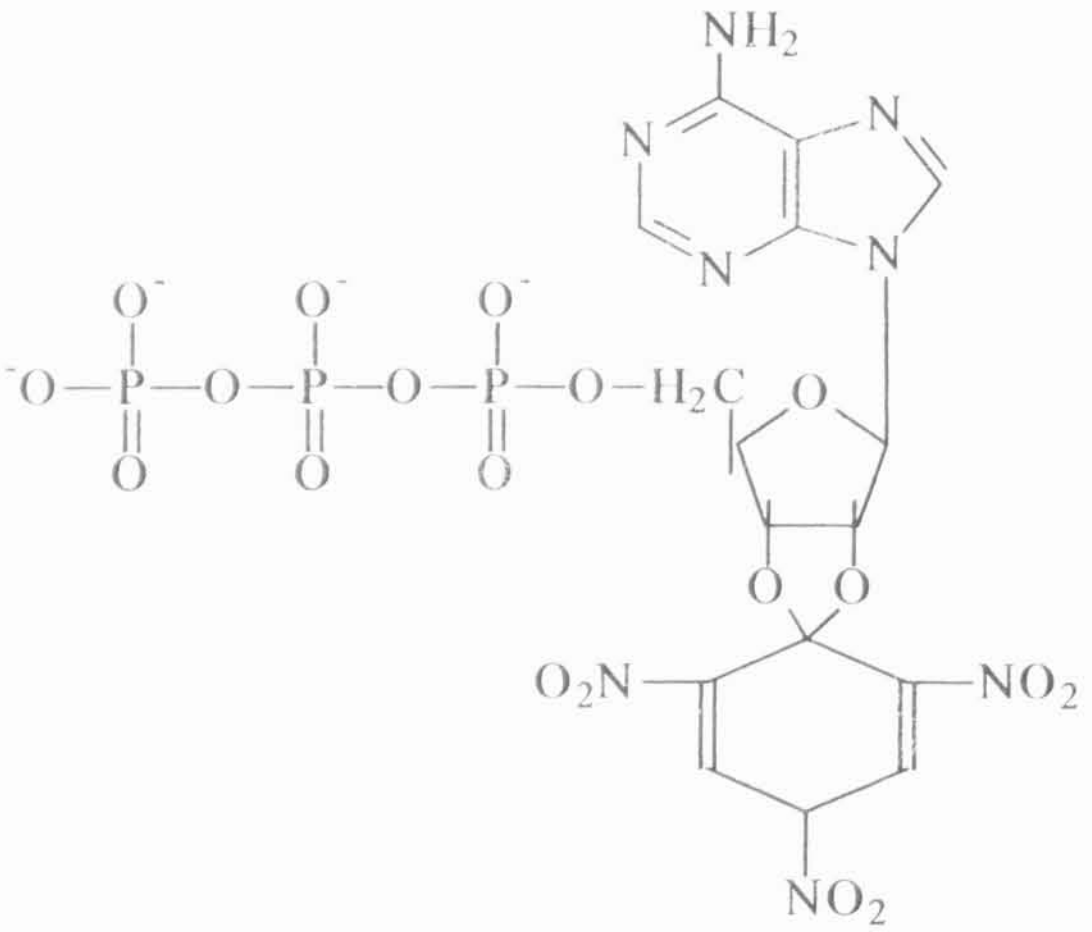

Fig. 14
2' (or 3')-O-(2,4,6-trinitrophenyl) adenosine 5'-triphosphate (TNP-ATP), the fluorescent analog of ATP.

When a dissociation constant for TNP-ATP is estimated one can easily estimate the dissociation constant for ATP. This is achieved by the measurement of the changes in emission spectra of TNP-ATP during the competitive displacement of ATP by TNP-ATP.

7.1.1. TNP-ATP Binding.

The signal of buffer (1 mL of 50 mM Tris-HCl) and buffer containing 1.6μM protein was collected before the addition of TNP-ATP (purchased from Molecular Probes, USA), and this value was subtracted from all further raw data as a background. Aliquots of TNP-ATP were subsequently added to samples. The mixtures were gently stirred, and the fluorescence intensity was recorded. Dilution corrections of the protein and probe concentrations were calculated. The fluorescence intensity was normalized so that the fluorescence intensity of a 1 μM free probe was set to unity. The dependence of normalized fluorescence intensity on the TNP-ATP concentration was fitted to the equation (Kubala 2003)

$$F^{*} = [P]_T + \frac{\gamma - 1}{2}\left([P]_T + [E]_T + K_P - \sqrt{([P]_T + [E]_T + K_P)^2 - 4[P]_T[E]_T}\right), \qquad [1]$$

where F is the normalized fluorescence intensity, $[P]_T$ is the concentration of TNP-ATP, $[E]_T$ is the concentration of the protein, γ is the fluorescence intensity enhancement factor of the bound probe relative to the free probe, and K_P is the dissociation constant. The fluorescence intensity enhancement factor γ, which is the ratio of respective quantum yields of bound to free probe, was estimated to be $\gamma = 2.3 \pm 0.2$. All the parameters except K_P were kept constant during the fitting procedure. The K_P values are presented as a mean ± SEM from at least three independent measurements.

Formula [1] can be extended to proteins with n identical and non-cooperative binding sites per protein molecule as follows (Kubala 2003):

$$F^{*} = [L]_T + \frac{\gamma - 1}{2}\left([L]_T + n[E]_T + K_P - \sqrt{([L]_T + n[E]_T + K_P)^2 - 4n[L]_T[E]_T}\right). \qquad [2]$$

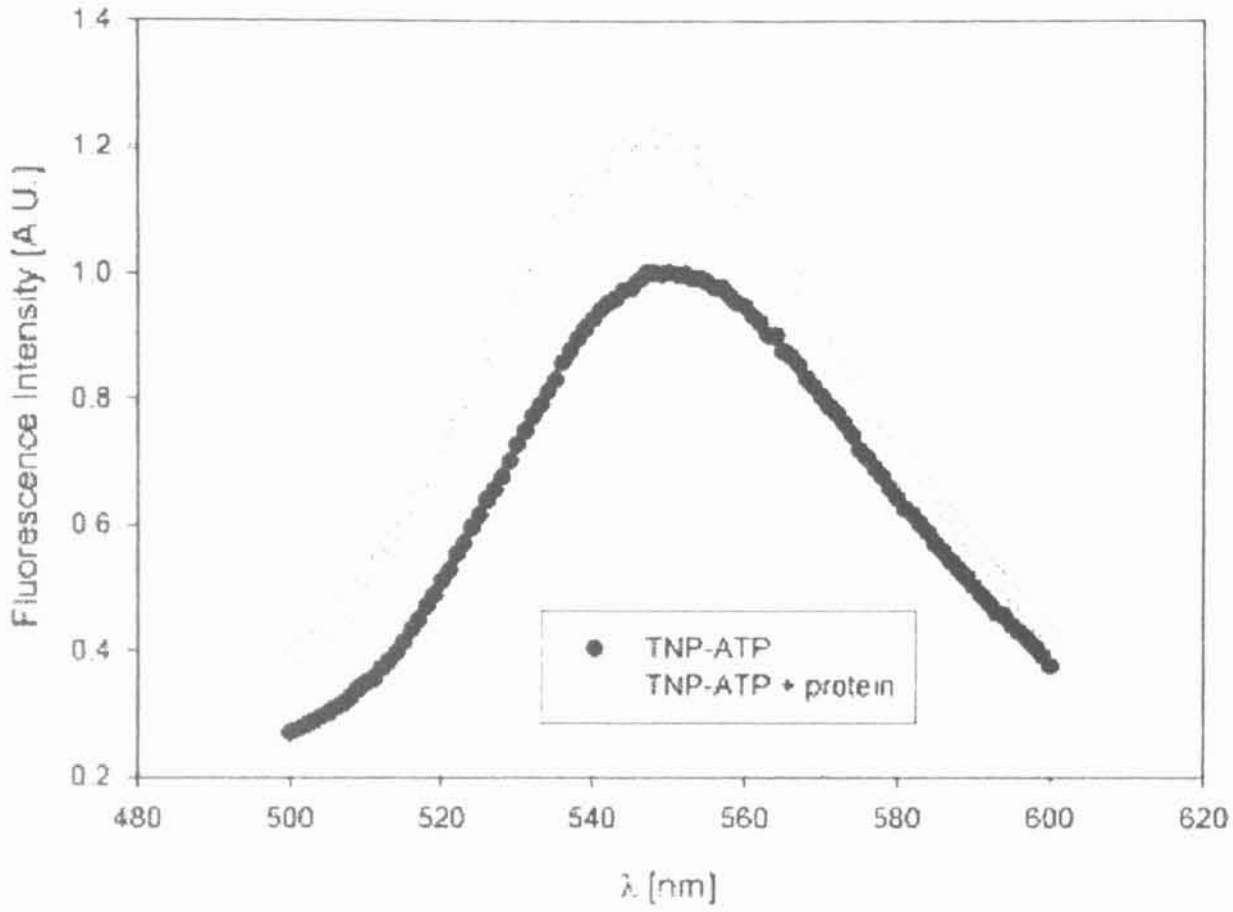

Fig. 15
TNP-ATP emission spectra in the absence (black dots), and in the presence of the WT protein (white dots). TNP-ATP, a fluorescent analog of ATP, is sensitive to the polarity of its micro-environment. Binding of this dye to a protein can be thus detected by monitoring the changes in emission spectra, a blue shift and an enhancement of the intensity of fluorescence.

7.1.2. Competitive Displacement of TNP-ATP by ATP

ATP was purchased from Sigma-Aldrich (Germany). The experimental procedure was the same as for TNP-ATP binding, except that titration was performed in 1 mL of 50 mM Tris-HCl containing 20 mM ATP, pH 7.5. ATP is a weak acid and in high concentration can cause a substantial shift of pH; therefore, pH was adjusted by titration with HCl only after addition of ATP. ATP competitively displaced the TNP-ATP from the binding sites, resulting in the lower fluorescence intensity as compared to that of the titration in the absence of ATP. The signal of buffer and protein (if present) was collected before the addition of TNP-ATP, and this value was subtracted from all further raw data as a background. Dilution corrections of the protein and probe concentrations were calculated. The fluorescence intensity was normalized as described above. The dependence of normalized fluorescence intensity on the concentration of TNP-ATP was fitted to the equation (Kubala 2004)

$$F^{*} = [P]_T + \frac{\gamma - 1}{2}\left([P]_T + [E]_T + K_P + [A]_T \frac{K_P}{K_A} - \sqrt{([P]_T + [E]_T + K_P + [A]_T \frac{K_P}{K_A})^2 - 4[P]_T[E]_T}\right), \quad [3]$$

which describes the situation where probe and ATP compete for the same binding site. $[A]_T$ is the total concentration of ATP, and K_A is the dissociation constant for ATP. All the parameters except K_A were kept constant during the fitting procedure. The K_P value was calculated as described above. All the K_A values are presented as the mean ± SEM of at least three independent measurements.

All TNP-ATP fluorescence intensity measurements were performed at room temperature (22 °C) using the FluoroMax-2 (Jobin Yvon/Spex) steady-state fluorometer, in 0.4 x 1 cm quartz cuvettes. Excitation and emission wavelengths were set to 462 and 527 nm, respectively. Both the excitation and emission bandpasses were 10 nm, and the integration time was 5 s.

7.2. FITC and Eosin Fluorescence Measurements

The FITC fluorescence anisotropy measurements as well as the eosin steady state fluorescence measurements were performed to investigate the rigidity of the N-domain of the Na^+/K^+ ATPase. In order to obtain pure N-domain, which is required for time resolved studies, we had to cleave the N-domain – GST fusion protein and remove the GST.

GST fusion protein L354–P588 (15 μM) in 20 mM Tris/HCl, pH 9, was labeled for 30 min with 30 μM FITC in dark at room temperature. Residual free FITC was removed by dialysis over night against a large excess of 50 mM Tris/HCl, 150 mM NaCl, 2.5 mM $CaCl_2$, pH 7.8. The GST tag was split off by 10 U of human thrombin per mg of GST fusion protein for 1 h at room temperature with gentle shaking. The GST protein was removed by incubation of the mixture with 1 mL of pre-equilibrated glutathione Sepharose (see the Molecular Biology section). This procedure was repeated twice. Finally, thrombin and buffer components were removed by size exclusion chromatography on a 3 mL Sephadex G-25 column preequilibrated with 20 mM Tris/HCl, pH 7.8. The concentration of the FITC labeled loop was 145 μg/mL (2.88 μM), the molar ratio of FITC bound to peptide was 1.2.

Steady-state fluorescence anisotropy of FITC-labeled N-domain was measured in L-format using the PerkinElmer LS50B fluorometer. The excitation and emission wavelength was 480 nm and 525 nm, respectively. The excitation and emission bandpasses were 5 nm, and the integration time was 1 s.

The excited state lifetime and the anisotropy decay measurements were performed with the K2 Phase-Domain fluorometer in L-formate with the modulation frequencies ranging from 10 MHz to 200 MHz (the excitation wavelength was set to 480 nm). A filter in the emission channel was used instead of the emission monochromator. Data analysis was performed using a K2 software.

Eosin Y is a fluorescence label competing with ATP for its binding site in the membrane-embedded enzyme. It has been used to demonstrate ATP competition as well as Mg^{2+} and K^{+} induced conformational changes in Na^{+}/K^{+} ATPase (Skou 1988, 1983, Esmann 1994). Interaction of eosin Y with GST fusion proteins was studied according to Skou & Esman (1988) in 20 mM Tris/HCl, pH 7.8, at 37 °C. Excitation (480–530 nm with λ_{em} = 538 nm) and emission (530–580 nm with λ_{exc} = 518 nm) spectra in the presence of 1 μM or 10 μM (L354–P588)–GST fusion protein, and GST-free controls, were recorded on a Hitachi F-3000 Fluorescence Spectrophotometer with 5 nm bandpass. Steady-state fluorescence studies were performed with the (L354–I777)–GST fusion protein in the same buffer at 37 °C on a PerkinElmer LS50B Luminescence Spectrometer exciting the probe at 518 nm and recording the emitted fluorescence at 530 nm (5 nm band passes each) and using an emission filter of 530 nm. The following ligands were tested with respect to their influence on the steady-state fluorescence of 100 nM eosin Y in 20 mM Tris/HCl, pH 7.8, in the presence of the H4-H5 loop: 10 mM Na^{+}, 5 mM Mg^{2+}, 5 mM PO_4^{3-}, 1.5 mM and 3 mM ATP. The largest construct, the (L354–I777)–GST fusion protein, and the C-terminally shortened construct L354–P588 were used for a comparative study.

8. Results and Discussion

8.1. Studies on the Structural Stability of the N-domain by FITC Anisotropy Decay and Eosin Fluorescence

8.1.1 Motivation

Following the SERCA analogy, the N-domain of the Na^+/K^+ ATPase should bend towards the the P-domain upon the binding of ATP (Chapter 3.2). This process may thereby also explain the amino acid labelling of the P-domain revealed by experiments with 8-N_3-TNP-ADP (Ward 1998). The same consideration may apply to the labelling of P668 by 4-N_3-2-NO_2-phenylphosphate (Tran 1996). It was therefore justified to learn more about the rigidity of the N-domain. This issue was investigated by FITC fluorescence anisotropy decay and lifetime measurements as well as by steady-state eosin fluorescence studies.

8.1.2. Results

FITC labeled L354–P588 loop protein with a molar ratio of fluorophore/protein of 1.2 was prepared as described in the Chapter 7.2. Its steady-state fluorescence anisotropy of $r = 0.25$ was quite high for a soluble protein, indicating a low flexibility in the N-domain. This value is, however, significantly lower than the $r = 0.34$ of the FITC labeled Na^+/K^+ ATPase in membranes (Amler 1992). Additionally, to get a deeper insight into the rigidity of the FITC-labeled L354–P588 H4-H5 loop, the excited state lifetime and anisotropy decay of the FITC-labeled protein fluorescence were determined using a phase domain fluorometer as described in Chapter 7.2. We found a two-component fluorescence intensity decay with the major lifetime component $s_1 = 3.5$ ns ($f_1 = 0.77$) and the minor component $s_2 = 1.7$ ns ($f_2 = 0.23$). The corresponding average lifetime of the excited state was determined as $s = 3.1$ ns.

The anisotropy decay of FITC-labeled L354–P588H4-H5 loop was determined in L-format. A two-component decay with a larger component of $q_1 = 11.3$ ns and a shorter component of $q_2 = 1.2$ ns, seemed to satisfactorily fit the collected data.

In contrast to results reported for the membrane-embedded Na^+/K^+ ATPase (Skou 1988; Esmann 1994), we observed no change in the excitation or in the emission fluorescence spectra of eosin Y in the presence of any of H4-H5 loop–GST fusion proteins. No effect of Na^+, Mg^{2+}, PO_4^{3-} or ATP on the eosin Y steady-state fluorescence was seen in the presence of 1 μM GST fusion protein L354–I777.

8.1.3. Discussion

Former studies with pyrene isothiocyanate indicated a rigid structure of the ATP binding site in the membrane embedded sodium pump (Linnertz 1998). Conformational stability of the N-domain is also evident from the high steady-state fluorescence anisotropy of r = 0.25 for the FITC-labeled H4-H5 loop and from its long anisotropy decay of q_1 of 11.3 ns. The shorter component of the anisotropy decay (q_2 = 1.2 ns) is short enough to be ascribed to the wobbling of the fluorophore around its binding site. The longer component (q_1 = 11.3 ns), on the other hand, is long enough to reflect the motion of the whole FITC-labeled H4-H5 loop and not only segmental motions, favoring the view that the whole loop tumbles in solution.

Additional support to this conclusion comes from the fact that, in contrast to the membrane-embedded Na^+/K^+ ATPase, the loop alone when stained with eosin does not respond to addition of ATP, Na^+ or Mg^{2+} by fluorescence changes (Skou 1988). The finding that there is no influence of ligand binding to the GST fusion proteins on the eosin Y steady-state fluorescence is rather surprising because Costa et al. reported on an eosin interference with MgATP in the dimer formation of a H4-H5 loop protein of Na^+/K^+ ATPase (Costa 2003). However, it seems to support a conclusion that the N-domain of the isolated H4-H5 loop is unable to twist down to the P-domain (Jorgensen 2003). Such a conformational change is needed in the membrane embedded Na^+/K^+ ATPase to enable both, 8-N_3-TNP-ADP (Cavieres 2000) and 4-azido, 2-nitro-phenylphosphate (Tran 1996) to label the P-domain at an amino acid C-terminal of K736 (Cavieres 2000) and at P668 (Tran 1996).

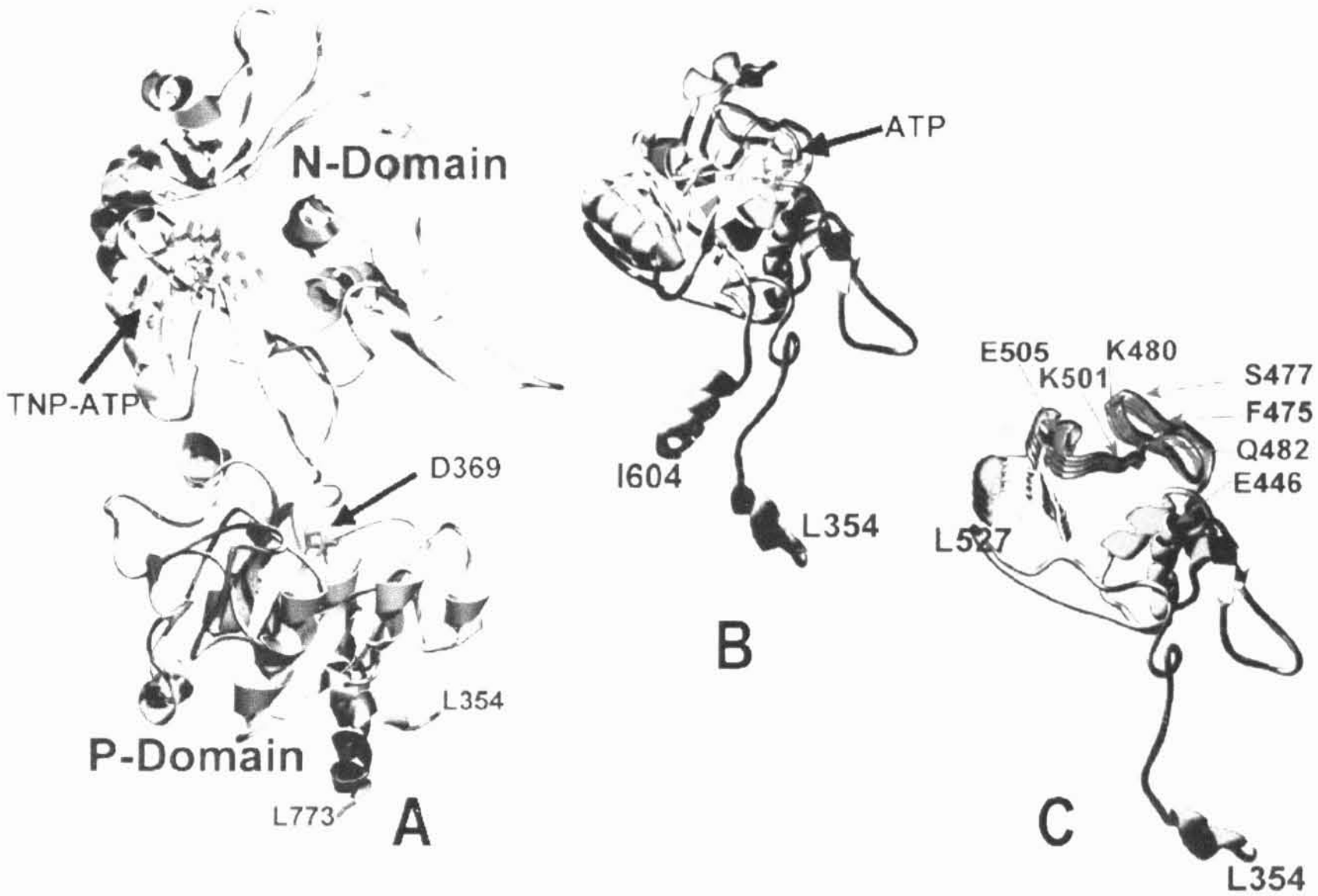

Fig. 16
C-Terminal truncation of the H4-H5 loop leads to loss of TNP-ATP binding due to unfolding of the N-domain as revealed by molecular modelling. (A) The complete H4-H5 loop starting at L354 and ending at L773 contains the N-domain interacting with TNP-ATP and the P-domain (D369 shown in blue). (B) The size of the isolated H4-H5 loops shortened by the C-terminal part of the P-domain to L354–I604 is without effect on TNP-ATP binding. (C) The stability of the N-domain and its ability to bind TNP-ATP is lost, however, when the sequence C-terminally of L527 is removed, although all the amino acids known to interact directly with ATP, and shown in purple are still present (E446, Q482, F475, S477, K480, K501, E505). The mobility of the structure in the residual N-domain of L354–L527 forming the ATP binding site is indicated by red arrows.

Neither method provided any indication of a conformational change of the N-domain upon ligand binding in the investigated GST fusion protein. It is thus very likely that the N-domain of the isolated loop forms a rigid structure, unless essential parts of the backbone are removed (Fig. 16). Consequently, we can conclude that the N-domain containing the ATP-binding site is a rigid structure, without flexible segments.

8.2 Truncation of the Cytoplasmic H4-H5 Loop of the Na^+/K^+-ATPase α-subunit and the TNP-ATP Binding

8.2.1 Motivation

Molecular modelling of the H4-H5 loop of the Na^+/K^+-ATPase according to the E1-Ca^{2+} ATPase (Ettrich 2001) revealed the N- and P-domain structures that has been almost identical with those found with X-ray crystallography and NMR analysis (Hakanson 2003; Hilge 2003). In silico docking of ATP and TNP-ATP to the H4-H5 loop showed a single ATP binding site only (Kubala 2003) (Fig. 16). In this active site residing between I390 and L576 (Table 1), eight amino acids interact with ATP (Kubala 2003).

To ensure that the docking experiments reflect actually the properties of the loop in solution, we analyzed TNP-ATP equilibrium binding to the (L354–I777)–GST fusion protein that contains both the N-domain and P-domain. Experimental titration result were fitted to theoretical curves (Chapter 7.1.1), describing the TNP-ATP binding for one [1] and two [2] binding sites in order to assess the number of binding sites on the H4-H5 loop.

Further means to search for a second ATP binding site was the preparation of several shorter loop constructs. Consequently, a number of GST fusion proteins starting at L354 and ending at varying C-terminal ends were expressed and purified. Their abilities to bind TNP-ATP were measured and analysed.

Amino terminal shortening of the loop protein was tested as well. We prepared the construct I390–S601 that lacks the phosphorylation site at D369. With these constructs the same measurement and analysis procedure was performed as with the C-terminal shortening ones.

8.2.2 Results

The TNP-ATP titration experiment with the (L354–I777)–GST fusion protein revealed that TNP-ATP binds to a single site only. Fitting of the fluorescence enhancement to both theoretical curves [1, 2], the single site nucleotide binding model and the binding model for two binding sites (Fig. 17), gave no indication for a second site.

The constructs without the C-terminal part of the P-domain showed unaltered K_D values of the H4-H5 loop–TNP-ATP complexes oscillating around a mean value of 3.35 μM (Table 1). The TNP-ATP binding properties changed drastically, however, when C-terminal shortening down to L527 removed those parts of the N-domain that apparently stabilized its backbone (Fig. 16). We observed an approximately 40% increase of the dissociation constant K_D for the shortened construct, L354–L541 (K_D = 4.73 μM), but a sharp significant increase of the K_D for TNP-ATP for the shortest construct, L354–L527 (200%, K_D = 10.05 μM; Table 1). We should add that shorter constructs could not be purified because they showed an increasing tendency to precipitate in solution. This shortest construct L354–L527 still contained all amino acids known to be necessary to bind ATP (Fig. 16) (Chapter 3.1.1.1.).

The N-terminal shortened construct (I390–S601) showed a single TNP-ATP binding site as well. The protein had the same TNP-ATP binding properties as the longest protein L354–I777 with K_D = 3.50 μM (Table 1).

Amino acid sequence or mutation	Length/amino acids (without GST)	TNP-ATP Binding	
		K_D (μM)	
		Mean	SEM
L354-L777	324	3.55	0.35
L354-I604	251	3.3	0.06
I390-S601	212	3.5	0.07
L354-P588	235	2.95	0.05
L354-L576	222	3.6	0.07
L354-L541	188	4.73	0.19
L354-L527	174	10.05	0.95
N398D (L354-I604)	251	3.3	0.2
D369A (L354-I604)	251	3.5	0.5

Tab. 1
TNP-ATP binding to H4-H5 loop–GST fusion proteins of different lengths. K_D values were calculated using equation [1]. The number of binding sites for ATP for a H4-H5 loop was considered 1 for all investigated proteins. Mean values ± SEM are given at least for six independent experiments.

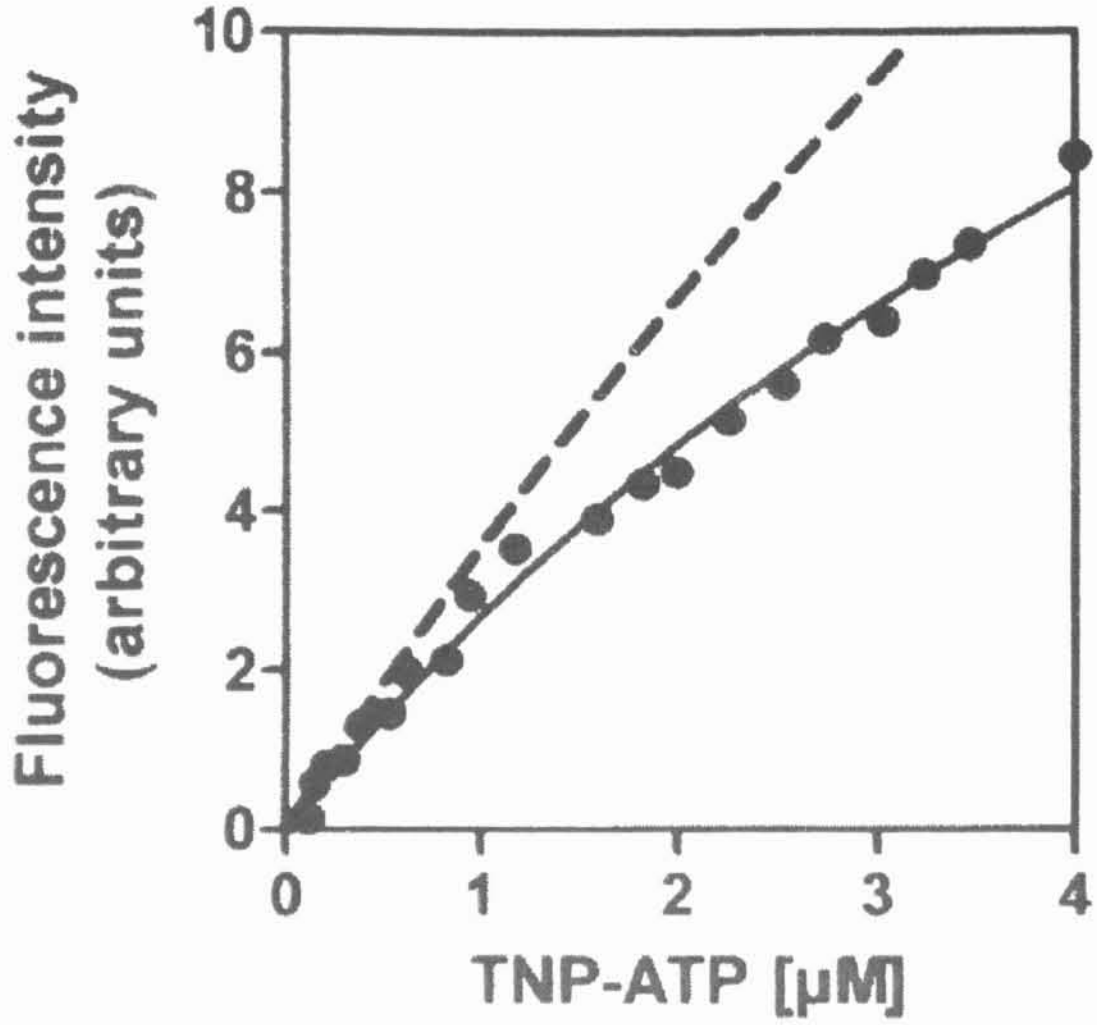

Fig. 17
Binding of TNP-ATP to the (L354–I777)–GST fusion protein, and fit of the data to equations for 1 or 2 TNP-ATP binding sites. The (L354–I777)–GST fusion protein (1.6 μM) was titrated with TNP-ATP in 50 mM Tris/HCl, pH 7.5 at 37°C. Regression analysis according to the equations [1] and [2] (solid line: equation [1]; broken line: equation [2], for n=2; also Table 1).

8.2.3 Discussion

The interpretation of the above reported data on the truncation of the H4-H5 loop is considerably facilitated by the availability of a molecular model (Ettrich 2001). Unfortunately, the structure of the H4-H5 loop seems to vary depending on the presence of the phosphorylation domain as is apparent from the following example. The model based on the E1 crystal structure of Ca^{2+} ATPase (Toyoshima 2000) and respecting the N- and C-terminal parts of the P-domain (Ettrich 2001), shows F548 as part of the ATP site (Fig. 18A). On the other hand, in the model based on the crystal structure of the N-domain of Na^{+}/K^{+} ATPase and not including the P-domain (Hakanson 2003) (Fig. 18B), F548 is buried under the surface of the ATP site. The role of F548 on the ATP and TNP-ATP binding has been investigated earlier (Kubala 2003, Hofbauerova 2003, 2002). The effect of mutation of this specific amino acid on the nucleotide binding property of the isolated H4-H5 loop is rather drastic (Kubala 2003). It remains, however, unclear whether F548 directly interacts with ligands or whether its importance

is just in the formation of the structural backbone of the ATP binding pocket. The adjacent amino acid residue C549, can be labeled by erythrosine isothiocyanate in the membrane embedded Na^+/K^+ ATPase after blocking of the E1 ATP binding site with FITC (Linnertz 1998). In the H4-H5 loop model of Na^+/K^+ ATPase (Ettrich 2001) obtained analogously to E1-Ca^{2+} ATPase (Toyoshima 2000), F548 is part of the ATP binding site and C549 is also accessible. However, in the crystal structure derived exclusively from the N-domain (Hakanson 2003), both amino acids are hidden under the surface as part of the structural backbone. It seems therefore, that the model respecting the P-domain-forming peptide extensions of the N-domain (Ettrich 2001) fits better to these experimental findings.

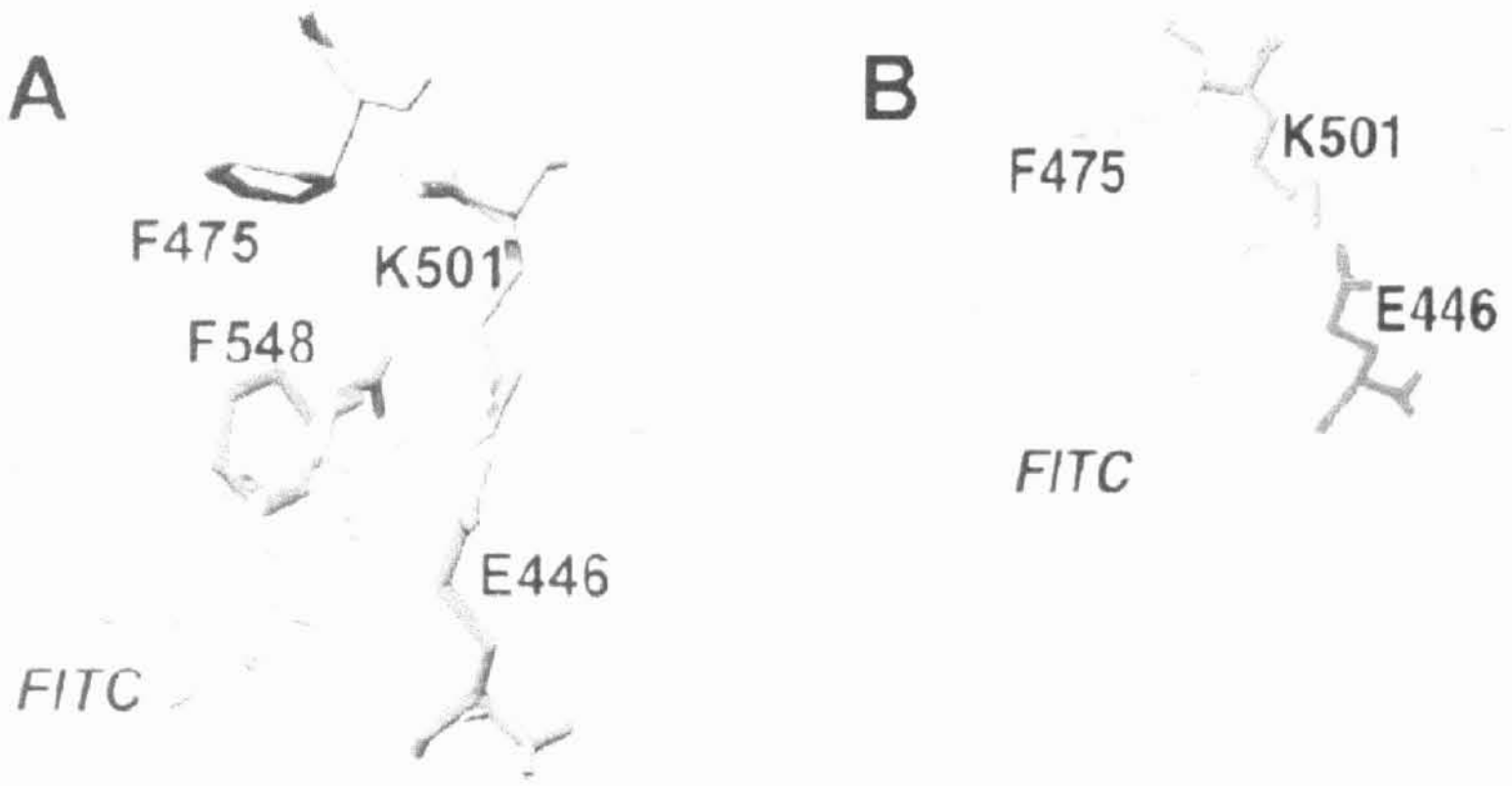

Fig. 18
Recognition of FITC by amino acids forming the ATP binding site of the N-domain. (A) Model of the whole loop in analogy to the E1-Ca^{2+} ATPase structure (N- and P-domains, L354–L773). Covalent coupling of FITC to K501 is accomplished by a hydrophobic interaction of the benzoyl-group within FITC with F548. (B) Model based on the N-domain crystal structure of α_2 Na^+/K^+ ATPase (N-domain only, R378–D586). F548 is buried under the surface of the protein and therefore not able to interact with ligands in the nucleotide binding pocket.

Molecular modelling of the truncated H4-H5 loop revealed that a big part of the N-domain can be removed without decreasing the TNP-ATP binding properties (compare Table 1 with Fig. 16). The increase in K_D value of the TNP-ATP protein

complex as found upon the extreme C-terminal shortening to the L354–L527 construct, could be analyzed by dynamic and energy minimization runs, and attributed to the increased mobility of certain parts of the loop structure (Fig. 16).

Consistent with recently reported data on NMR analysis (Hilge 2003), TNP-ATP binding studies (Gatto 1998, Kubala 2003) and in silico docking experiments (Ettrich 2001), the above reported data indicate (Figs 16 and 17, Table 1) that the isolated H4-H5 loop of Na^+/K^+ ATPase contains a single ATP site only. Former reports on the existence of two ATP binding sites on both, the N-domain and P-domain (Tran 1996, Cavieres 2000) in the membrane embedded sodium pump should therefore be re-interpreted in terms of the existence of other protein conformations (Thoenges 1997, 1999) differing from that of the isolated H4-H5 loop in solution.

8.3 Structure of the ATP Binding Site

8.3.1 Motivation

NMR study of isolated Thr^{357}-Leu^{600} segment of SERCA (corresponding to the N-domain) showed that Glu^{439}, Ser^{488} and Val^{514} are influenced by nucleotide binding (Abu Abed 2002); corresponding residues in Na^+/K^+-ATPase are Asp^{443}, Ser^{477} and Met^{500}, respectively. Moreover, Fe^{2+}-oxidative cleavage of Na^+/K^+-ATPase suggested that Asp^{443} plays an important role in ATP binding to and/or phosphorylation of the enzyme (Patchornik 2002). The homology modelling of the H_4-H_5-loop predicted that Ser^{477} could participate in ATP binding (Ettrich 2001). Finally, Met^{500} is closely connected to the important Lys^{501}-Ala^{503} region. Using site-directed mutagenesis, we mutated Asp^{443}, Ser^{477} and Met^{500} to estimate the roles of these amino acids in ATP binding.

In our previous work (Kubala 2003) we reported, that the mutation of Arg^{423}, which is rather distant from the ATP binding site, resulted in a strong inhibition of both TNP-ATP and ATP binding (K_D(TNP-ATP) = 18 ± 2 μM and K_D(ATP) = 31 ± 10 mM). This was rather surprising because this residue is approximately 7Å from the bound molecule and lies outside the binding pocket. We proposed, hence, that Arg^{423} forms a hydrogen bond with Glu^{472} over a distance of 1.7 Å and that this hydrogen bond stabilizes the shape of the whole ATP binding pocket (Kubala 2003). Another distant residue, which could be important for the proper shape of the ATP binding pocket, is Pro^{489}, which is conserved among P-ATPases. To verify these hypotheses we performed also mutations of Glu^{472} and Pro^{489}.

The effect of these mutations was evaluated by the binding of TNP-ATP to the isolated N-domain containing the given point mutation. We estimated earlier that some mutations could affect only the TNP-ATP binding but not the ATP binding. Competitive displacement of TNP-ATP by ATP was therefore used to test the influence of the point mutation on the binding of pure ATP.

8.3.2 Results

All the mutants were expressed as GST-fusion proteins in *E. coli* and purified as described in Chapter 6. The purity of proteins was checked by 12% (w/v) SDS-PAGE. We observed a single band at 53 kDa (Fig. 13). The expression level was high for all mutants, except for the P489A one (Fig. 13). However, even in this case the synthesis was sufficiently high to perform all our experiments.

To verify that the GST protein itself does not bind TNP-ATP, the GST protein was incubated with TNP-ATP and the fluorescence was recorded. The fluorescence intensity of TNP-ATP in buffer did not change upon the addition of the GST protein. Thus, there was no significant binding of TNP-ATP to GST observed over the whole range of TNP-ATP concentrations used in our study. Accordingly, the GST-H4-H5-loop fusion protein was considered to be a suitable model system for studying the binding of TNP-ATP to the ATP-binding site. In contrast, incubation of all fusion proteins with TNP-ATP resulted in a clear and significant increase in fluorescence intensity compared to GST in buffer or buffer alone.

8.3.2.1 Binding of TNP-ATP to the GST Fusion Proteins

We confirmed our previous result (Kubala 2002) and estimated that the binding of TNP-ATP to the GST-[Leu^{354}-Ile^{604}] fusion protein (wild type) yielded the value of the dissociation constant $K_D = 3.1 \pm 0.2$ μM (Table 2). A new founding is that the M500A mutation did not significantly vary the results and also mutation E472A influenced the TNP-ATP binding only moderately. On the other hand, titration in the presence of E472A and S477A mutants resulted in a considerably smaller increase of fluorescence intensity as compared to wild-type. This difference suggests that the TNP-ATP binding was inhibited in these cases (Fig. 19). Even larger decrease was observed for the E472A mutant, and interestingly, further mutation of Arg^{423} (i.e. the R423LE472A construct) had no significant additional influence on this effect (Table 2). The most dramatic change was observed with the P489A construct; the TNP-ATP titration curve of this mutant was undistinguishable from that in the absence of any protein ($K_D > 100$ μM). The estimated dissociation constants values are summarized in the Table 2.

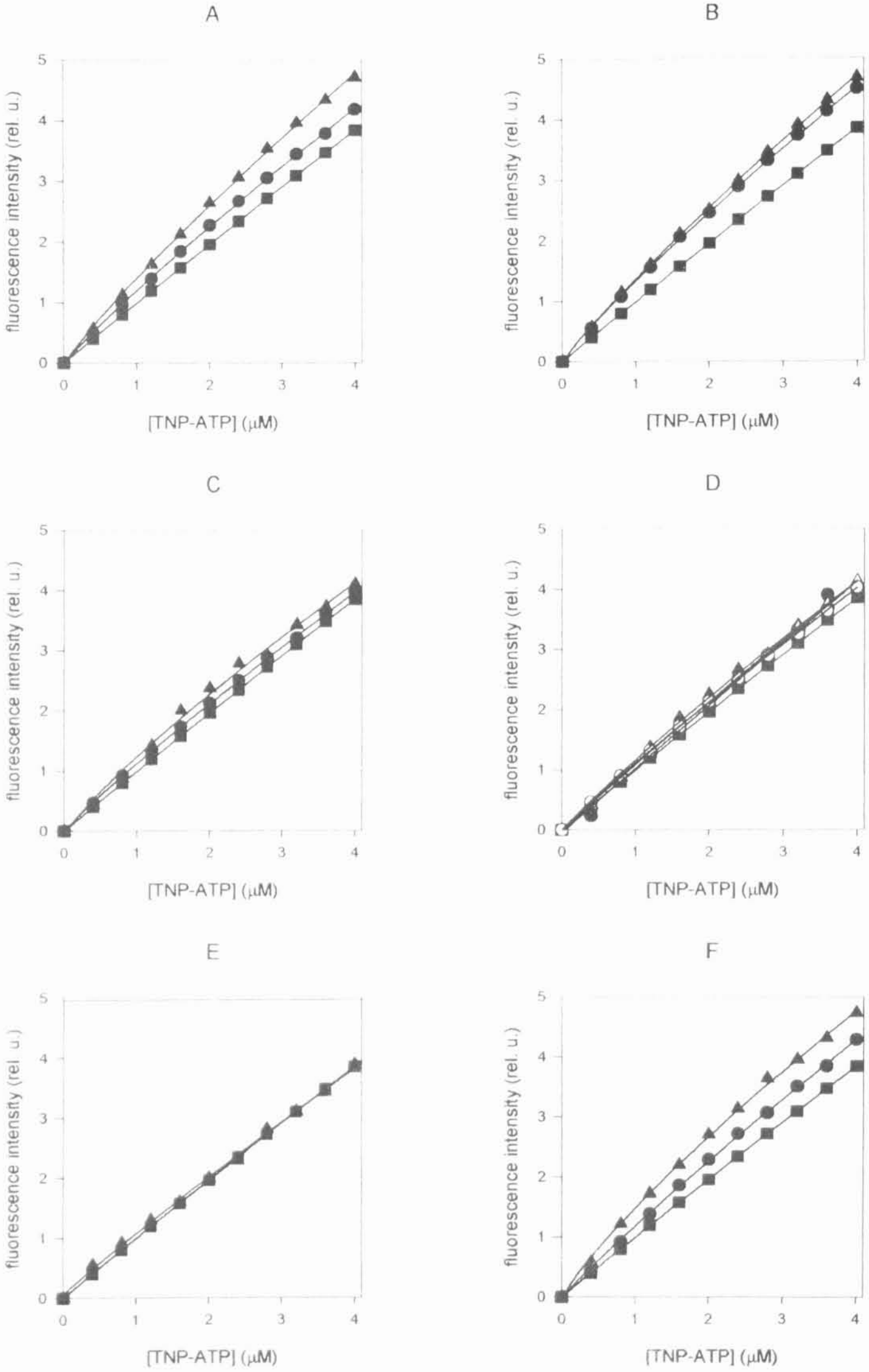

Fig. 19
TNP-ATP binding to the H_4-H_5 loop protein with point mutations in the presence and absence of ATP, respectively. GST fusion proteins (1.6 μM) containing point mutations (A: M500A; B: D443A; C: S477A; D: E472A; E: P489A; F: wild type) were titrated with TNP-ATP in 50 mM Tris-HCl, pH 7.5 (triangles) and in 50 mM Tris-HCl, 20 mM ATP, pH 7.5 (circles). For comparison, titration in pure buffer is shown (squares). Open symbols in graph D represent data for the double mutant R423LE472A.

Mutation	TNP-ATP Binding		ATP-Binding	
	K_D (μM)		K_D (mM)	
	Mean	SEM	Mean	SEM
wild type	3.1	0.2	6.2	0.7
D443A	3.7	0.2	32	8
R423L	18	2	31	9
E472A	15	4	20	11
R423LE472A	17	5	35	15
S477A	9	1	7	1
P489A	>100		not analyzed	
M500A	3.6	0.6	5	2

Tab.2
Dissociation constants for TNP-ATP and ATP binding to the GST- H4-H5 fusion proteins. The presented data are the average and SEM values from at least three independent measurements.

8.3.2.2 Binding of ATP to the GST Fusion Proteins

The dissociation constant of ATP binding to the H4-H5-loop of Na^+/K^+-ATPase is about three orders of magnitude higher than the one of TNP-ATP (Table 2). This suggests a certain stabilizing role of the trinitrophenyl moiety of the fluorescence probe in forming of the complex with protein. Hence, one has to admit that the interaction of the trinitrophenyl moiety itself with the ATP-binding site might affect the apparent K_D values found for our mutants. Therefore, we determined the dissociation constant of ATP-peptide complexes for all constructs as well.

Competition for the binding sites between ATP and TNP-ATP was used to characterize the binding of ATP to the fusion proteins. The presence of ATP in buffer (without any protein) did not influence the fluorescence intensity of TNP-ATP.

However, it has changed significantly the fluorescence intensity of TNP-ATP in the titration experiments performed in the presence of S477A and M500A mutants (Fig. 19). A lower fluorescence intensity in the presence of ATP indicated that some binding sites were occupied by ATP. This effect was much smaller in the presence of D443A and E472A mutants, suggesting that the ATP was bound to these mutants very weakly. Indeed, we observed an increase of the value of the dissociation constant 6.2 ± 0.7 mM estimated for the wild-type (Table 2) to 32 ± 8 mM for D443A and 20 ± 11 mM for E472A. In contrast, no significant change was observed with the mutations S477A (7 ± 1 mM) and S445A (5 ± 2 mM). The fact that mutant P489A didn't significantly interact with TNP-ATP disabled the estimation of the dissociation constant for the ATP binding in this case. The results of TNP-ATP- and ATP-binding to all mutants are summarized in Table 2.

8.3.3 Discussion

A part of the H4-H5 loop of Na^+/K^+-ATPase (sequence Leu^{354}-Ile^{604}) was used to test the influence of point mutations on the binding of ATP. TNP-ATP, the fluorescent analog of ATP, has been used to evaluate these changes in ATP binding in terms of TNP-ATP dissociation constants, as described in Chapter 7.1.

All residues were replaced by residues of similar or lower polarity. This can, in principle, increase the TNP-ATP microenvironment polarity within the binding pocket and, thus, influence the assessment of the dissociation constant. Fortunately, this effect is likely to be much less then the observed difference between K_D values for the wild type protein and most mutants. First, the ATP binding site is composed of eight amino acids, and thus, one point mutation can hardly cause a dramatic change in its polarity. Second, we performed model calculations to show that even a relatively large error in the γ value estimation would vary the dissociation constant for ATP only moderately; e.g., increasing the γ value from 2.3 to 4.5 would increase the calculated K_D (ATP) for E472A from 20 to 24 mM only. Therefore, we could treat the fluorescence enhancement factor as a constant for all the mutants.

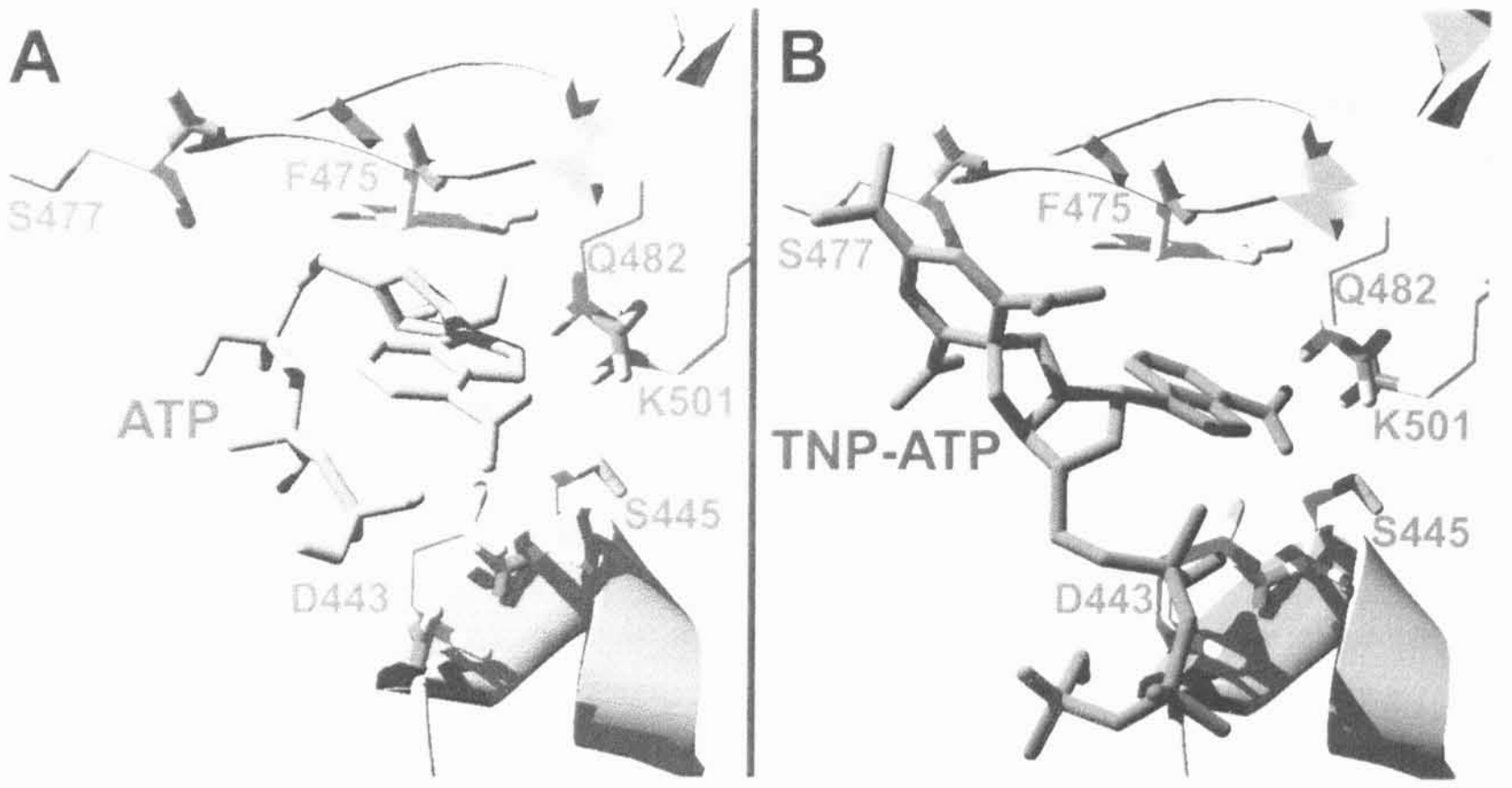

Fig. 20
Difference in binding between ATP and TNP-ATP. (A) The most important interactions in ATP binding are the aromatic stacking between the adenosine moiety and F475 and the hydrogen bonding of its NH_2 hydrogen donor with Q482 and D443. (B) The adenosine moiety of TNP-ATP is in the opposite position compared with ATP, and its NH_2 hydrogen donor lies too much in the back of the picture to form a hydrogen bond with D443.

The new model, based on the Hakanson's structure (Hakanson 2003), was used in computational docking experiments with free ATP and TNP-ATP. In silico docking experiments identified well the ATP binding site and resulted in the binding of both substrates. The actual power of our model to interpret the results of the studies of TNP-ATP and ATP binding to the H4-H5 loop (Table 2) needs to be tested further. Additionally, this model had to interpret by means of in silico docking experiments (Fig. 20) the observed changes in terms of interaction with specific amino acids (Table 2).

8.3.3.1 Hydrogen Bond Between Glu^{472} and Arg^{423}

To verify the hypothesis of the Glu^{472} - Arg^{423} hydrogen bond existence we mutated Glu^{472} to see whether this mutation would have an effect similar to that of the mutation of Arg^{423}. Indeed, a strong decrease of nucleoside triphosphate binding was observed for TNP-ATP (K_D = 15 ± 4 μM) and ATP (K_D = 20 ± 10 mM), and the values matched within the range of error values for Arg^{423}. Moreover, the performance of the R423L mutation on the construct already containing the E472A mutation (i.e. the double-mutant R423LE472A) did not bring any significant additional effect on both TNP-ATP (K_D = 17 ± 5 μM) and ATP (K_D = 35 ± 15 mM) binding, and again, the values match well the values obtained for the R423L mutant. Thus, we can see that these two mutations has no additive effect on the nucleotide binding, and this finding strongly supports the hypothesis that a hydrogen bond exists between Arg^{423} and Glu^{472} (Fig. 21). Such information is beyond the resolution of both N-domain structures mentioned above. Breaking this hydrogen bond leads to instability in the stretch of amino acids containing the residues Phe^{475}, Lys^{480} or Gln^{482} within the binding pocket, which are in proximity of the other residues involved in the ATP binding, such as Lys^{501} or Glu^{446}. This corresponds to our observation that mutations of Arg^{423} and Glu^{472} lead to a strong inhibition of Na^+/K^+-ATPase (Scheiner Bobis 1999).

8.3.3.2 The Pro^{489} Residue

Even more dramatic changes were observed after mutation of the conserved residue Pro^{489}. We were did not detect any TNP-ATP binding, suggesting that the performed

mutation substantially influenced the structure of the nucleotide-binding site. Indeed, Pro^{489} is located on the loop connecting the third and fourth β-strands of the N-domain (Fig. 22), and forms a kind of hinge between them. Proline is the only residue that forces the peptidic backbone to adopt the cis-conformation. Thus, the replacement of Pro^{489} by any other amino acid is expected to result in the change of the mutual position of the third and fourth β-sheets. The third β-strand contains residues Lys^{480} and Gln^{482}, while the fourth β-strand contains the segment Lys^{501}-Ala^{503}. Proper mutual position of these residues is required for the effective ATP recognition. Thus, the Pro^{489} mutation affects the backbone forming of the ATP binding site rather indirectly, similarly to what was discussed for Arg^{423} and Glu^{472} in the previous paragraph.

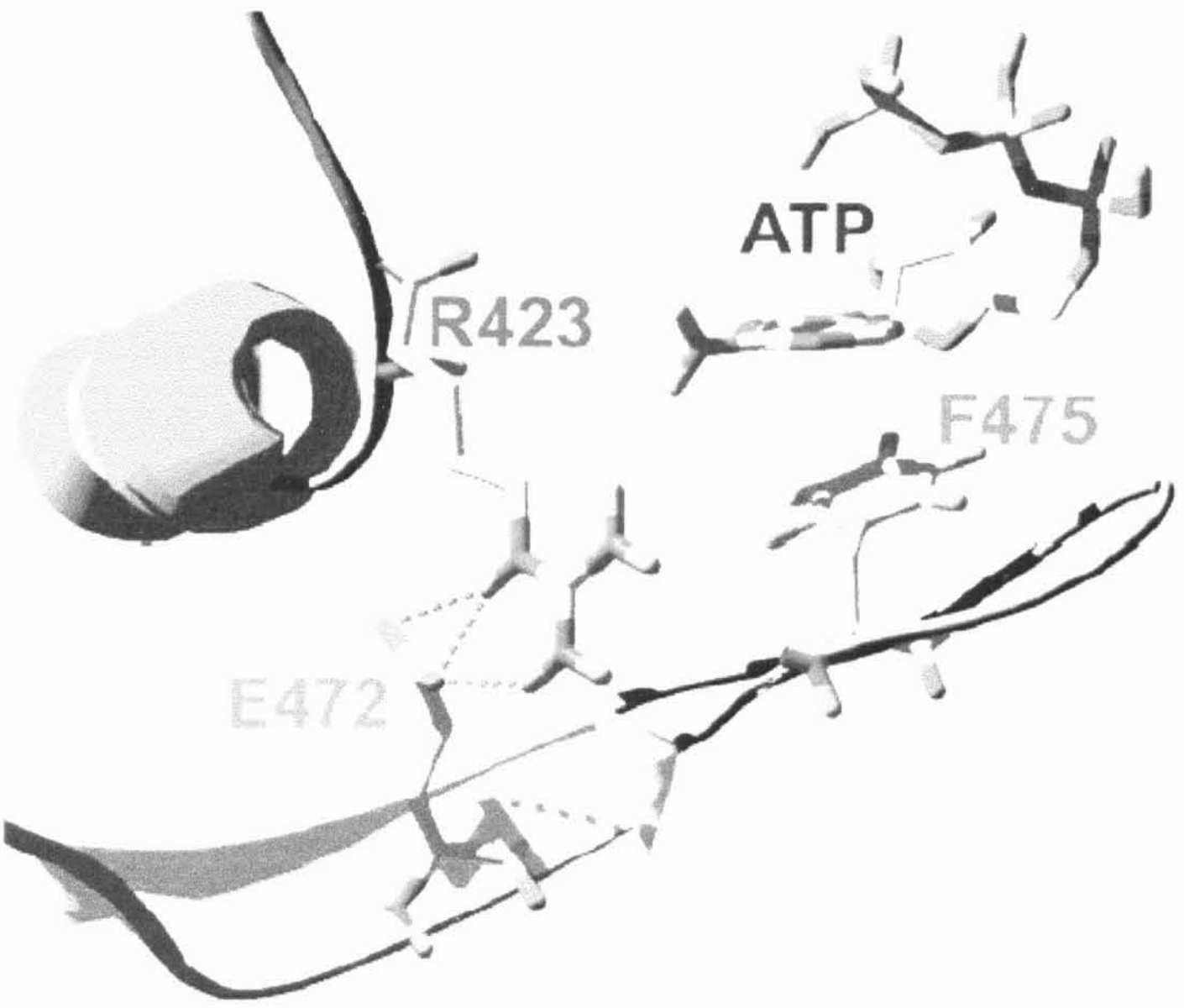

Fig. 21
Hydrogen bond between Glu^{472} and Arg^{423}. The shape of the ATP-binding pocket is supported by a hydrogen bond between Glu^{472} and Arg^{423} that brings the stretch of amino acids containing residues Phe^{475} and Glu^{482} (not shown) close to other residues involved in ATP binding, such as Glu^{446} and Lys^{501} (not shown).

8.3.3.3 Difference Between the ATP and the TNP-ATP Binding

Mutation of Ser^{477} resulted in a moderate change of the dissociation constant for TNP-ATP binding, whereas ATP binding was not affected at all (Table 2). Although this residue is localized more than 4.1 Å away from ATP, its closest distance to the Meissenheimer complex of TNP-ATP is only 2.5 Å. We conclude therefore that Ser^{477} interacts closely with the trinitrophenyl residue of the more bulky TNP-ATP.

However, such an argument failed in the case of the Asp^{443} mutation (Table 2), for which, we observed practically no difference in TNP-ATP binding, while the binding of pure ATP was strongly suppressed. In silico docking of both substrates revealed that the position of the ATP in the binding pocket is not precisely the same as the position of the adenosine triphosphate part of the TNP-ATP (Fig. 20). The aromatic stacking interaction between the adenosine moiety and Phe^{475} and hydrogen bonding of the adenosine NH_2 hydrogen donor were described to be the most important interactions of ATP and the protein (Kubala 2002; Kubala 2003a; Hilge 2003). On the basis of molecular modelling of both substrates in the binding pocket, we hypothesize the existence of the direct hydrogen bonding of the 6-NH_2 group of the adenine moiety with Gln^{482} and Asp^{443} in the case of ATP. It should be emphasized that three-dimensional fitting of the NMR structure and our model structure, both with bound ATP, shows that the adenosine NH_2 hydrogen donor in both structures is in nearly the same position, only 0.8 Å from each other. TNP-ATP, however, lies in a slightly different orientation in the binding pocket, and we are unable to observe hydrogen bonding of its 6-NH_2 hydrogen donor. Note that Asp^{443} is approximately 6 Å from the adenosine moiety in the NMR structure, which makes the direct interaction rather unlikely. However, if one compares the binding pocket of the crystal structure with that of both NMR structures, a discrepancy in the position of D443 (D450 in the NMR structures) is found. The carboxyl group of the D443 in the crystal structure is 2.7 Å from the position in the NMR structure without ATP and 3.4 Å with ATP. Moreover, recently published mutagenesis (Imagawa 2003) and iron-oxidative cleavage (Patchornik 2002) experiments suggested the importance of this residue for ATP binding. This discrepancy could reflect different transient subconformations of the protein and/or some segmental

dynamics. However, explanation of the discrepancy between the NMR structure and other experiments may need further investigation.

8.3.3.4 Met^{500} Residue - No Interactions with ATP

Mutation of Met^{500} altered neither TNP-ATP nor ATP binding. Although the peptidic backbone of this residue is 6.1 Å from the ATP molecule, its side chain is probably buried under the surface, and its mutation cannot influence the ligand binding (Fig. 22).

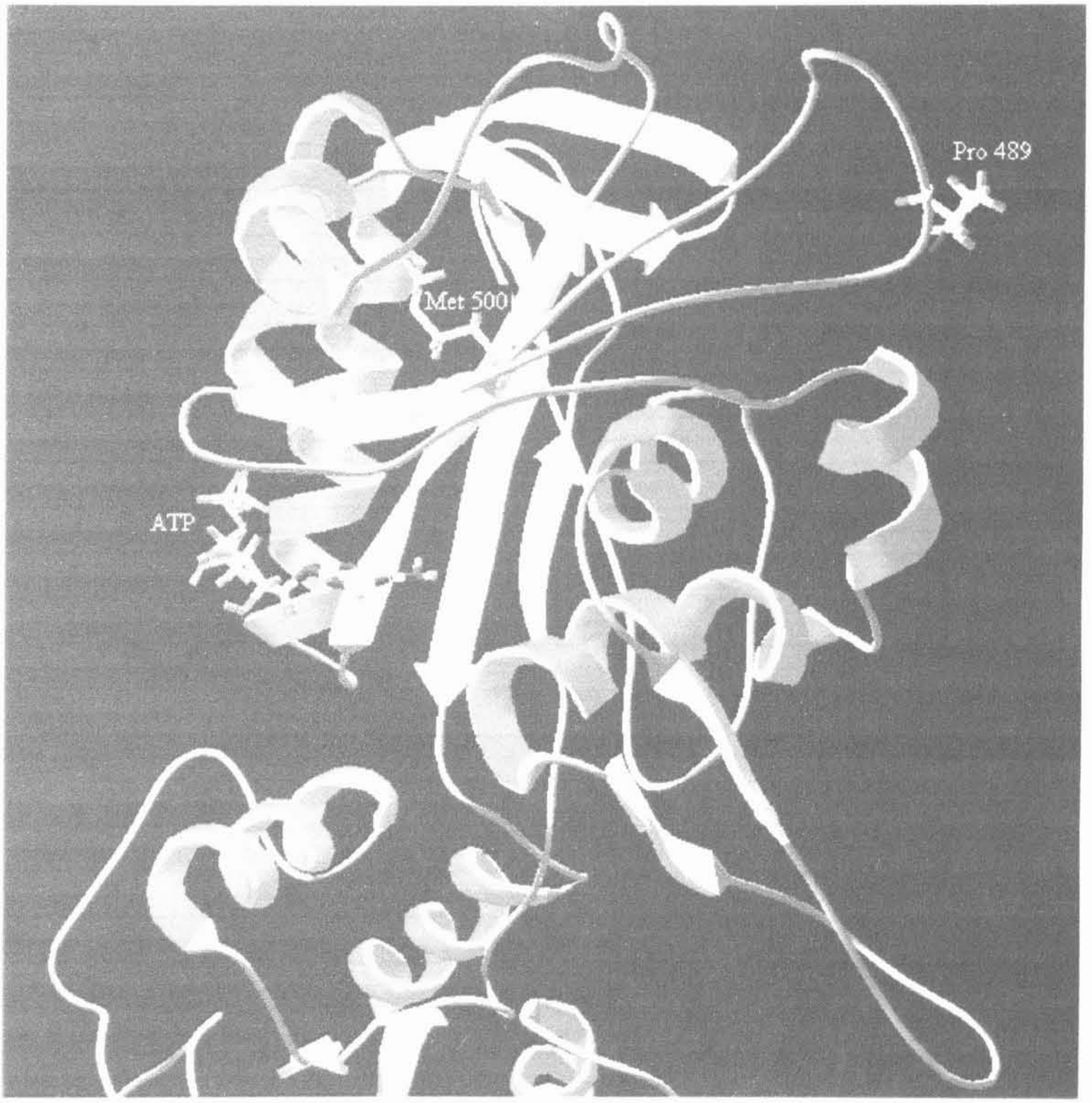

Fig. 22
N-domain of the H4-H5 loop with Pro^{489} and Met^{500} residues highlighted. Pro^{489} is located on the loop connecting the third and fourth β-strands of the N-domain, forming a hinge between them. Proline is the only residue that forces the peptidic backbone to adopt the cis-conformation and its mutation results in complete loss of ability to bind ATP. Side chain of Met^{500} is buried under the surface of the protein and its mutation does not influence the ATP binding.

9. Perspectives

9.1. Motivation

In order to obtain more information on the quartery structure of the Na^+/K^+ ATPase, on the possibility of the dimer formation and also on the conformational changes of the H4-H5 loop during the catalytic cycle, a new project is currently in progress. Its goals cannot be meet with the molecular biology methods we used for the characterisation of the ATP binding site, structural stability and the effects of the loop truncations. The main issue is the existence of the GST tag. GST is a relatively large protein approximately of the same size as the H4-H5 loop, and thus, when in the form of a fusion protein, can disable possible multimerization and/or conformational changes of the H4-H5 loop and their monitoring. The fusion protein can be cleaved by thrombin and the GST thereafter removed, as was done in the FITC anisotropy studies for the L354-P588 construct. However, for future experiments we considered not having the GST tag in our constructs at all, to be the easiest and most rigorous way.

This was achieved by subcloning the WT DNA to another expression vector, pET 21b. This vector contains the sequence coding the Kanamycin resistance, and the sequence coding the His tag – a sequence of 6 histidines, which fuses with our H4-H5 loop and is employed in the purification process in analogy with the GST. His tag is rather small in comparison with the GST and its effect on the H4-H5 loop multimerization and its monitoring can be neglected.

We chose the tryptophane fluorescence to be a measure of the conformational changes or dimerization. Tryptophane fluorescence is known to be sensitive to the polarity of its environment. Conformational change or a dimerization can be thus detected by a change in the emission spectra when an originally water-exposed tryptophane residue becomes buried in the hydrophobic protein environment or vice versa. The change in emission spectra can be correctly interpreted only if a single tryptophane residue signal is collected. Hence, it was essential to construct several single tryptophane mutants. There are two tryptophan residues within the wild type H4-H5 loop, i.e., W411 and W385 (Fig. 23). These tryptophane residues were mutated for phenylalanine residues, thus producing two different single-tryptophane mutants W411F and W385F, and no-tryptophane mutant W411FW385F. Having used this no-

tryptophane double-mutant as a template for other mutations, we obtained another set of single non-native tryptophan mutants: F404W, F571W, F426W, V684W, L733W, F683W, I627W and H496W. In this way, tryptophane residues were inserted into different parts of the H4-H5 loop where they perform like a "natural" fluorescent probe.

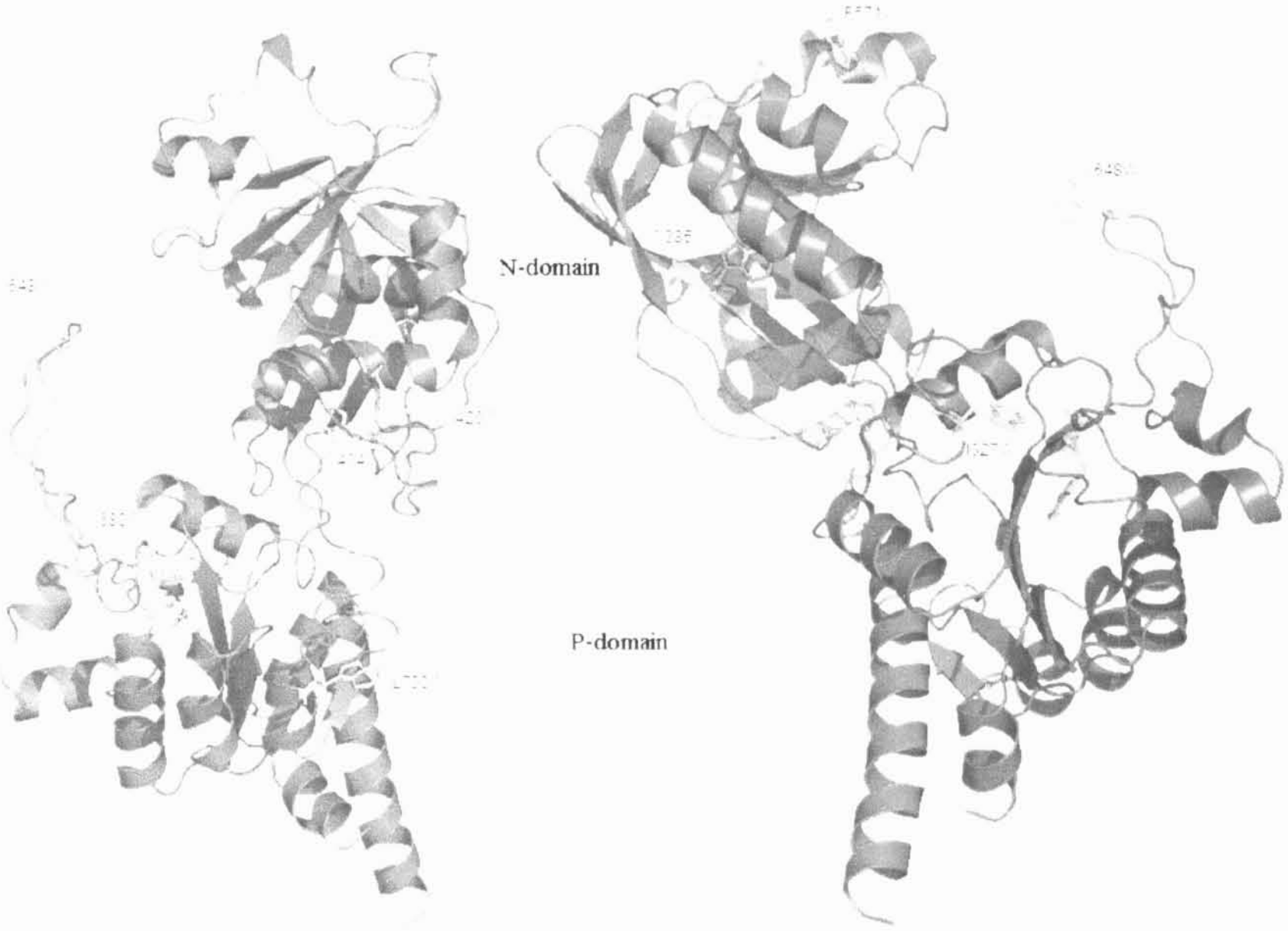

Fig. 23
Model of the H_4-H_5 loop (two different views). Both the natural and mutant positions of tryptophane residues are shown in red. The constructs, with a single tryptophan residue, were prepared and used in order to explore the conformational changes and the quaternary structure of the Na^+/K^+ ATPase.

9.2. Experimental Procedures and Preliminary Results

In order to induce and detect a dimerization or a conformational change of the single-tryptophane mutant, the sample was titrated by different ligands and the tryptophane fluorescence emission was recorded. Custom software was developed for the evaluation of emission spectra using the MatLab environment. The background was subtracted, the emission peak was fitted to a second order polynomial, and the position of the maximum of this curve was recorded. The titration curves were plotted in two different ways: (i) as the wavelength at the emission spectrum maximum versus the ligand concentration, and (ii) the fluorescence intensity versus the ligand concentration.

Results of the first experimental sequence show that several amino acid residues (W385, W411, W571, W627 and W683) exhibit a shift of the fluorescence maxima and, notably, the W627 and W683 residues exhibit the blue shift, which indicates that these particular amino acid residues are located within a segment that is buried upon the conformational change. Another, interesting hypothesis deals with a possibility that the particular amino acid resides in the contact site of the dimer during its formation. Unfortunately, we don't have enough information yet to make any conclusions.

Additional experiments are therefore to be performed. The first part of this future project will rely on the tryptophane fluorescence quenching. It is expected that the solvent-exposed residues will be quenched easier than the residues enwrapped within the core of the protein, thus providing similar information as the ligand titration experiments. The difference between the conformational changes and the dimerization will be thereafter explored by means of time resolved fluorescence spectroscopy. The anisotropy decay of the tryptophane fluorescence will be measured for particular mutants in the presence of the ligands and the distribution of the rotational correlation times will be computed. This will provide us a better insight in the changes in size and/or flexibility of the H4-H5 loop upon the ligand binding.

10. Conclusions

In this project we have analyzed the structural properties of the Na^+/K^+ ATPase and, in particular, characterized its ATP binding site. The overall stability of the N-domain of the H4-H5 loop of the Na^+/K^+ ATPase was examined by the means of steady state and time resolved fluorescence spectroscopy. Using the FITC anisotropy decay and eosin fluorescence we have shown that the N-domain of the H4-H5 loop forms a rigid structure without any flexible segments.

Using the tools of molecular modelling, we have built a model of the H4-H5 loop of the α-subunit of the Na^+/K^+ ATPase. This molecular model was used for the truncation experiments. The wild type sequence of the H4-H5 loop of the α-subunit of the Na^+/K^+ ATPase was trimmed from both, N- and C-termini and the ability of the truncated constructs to bind the TNP-ATP, a fluorescent analog of ATP, was tested in order to estimate the number and localization of the ATP binding sites. It was shown that there is only one ATP binding site residing on the N-domain of the H4-H5 loop of the Na^+/K^+ ATPase.

The molecular model of the H4-H5 loop of the Na^+/K^+ ATPase was also used to point out amino acid residues that might be involved in the ATP binding. These residues were mutated and the ability of these mutant constructs to bind the ATP was tested and compared to the wild type protein. TNP-ATP titration and competition experiments were used for the determination of the ATP binding. Apart from previously reported amino acid residues necessary for the ATP binding, we have found several amino acid residues that support the overall form of the ATP binding site and we have confirmed that the hydrogen bond between Glu^{472} and Arg^{423} is essential for the maintenance of the proper shape of the ATP binding pocket. Using the in silico docking procedure we have also pointed out the difference between the ATP and TNP-ATP binding to the ATP binding site of the Na^+/K^+ ATPase.

11. References

Abu-Abed M, Mal TK, Kainosho M, MacLennan DH, and Ikura M (2002) Characterization of the ATP-binding domain of the sarco(endo)plasmic reticulum Ca(2+)-ATPase: probing nucleotide binding by multidimensional NMR. Biochemistry 41: 1156-1164

Amler E, Abbott A, Ball WJJ (1992) Structural dynamics and oligomeric interactions of Na,K ATPase monitored using fluorescence energy transfer. Biophys J 61:553-568

Antolovic R, Bruller HJ, Bunk S, Linder D and Schoner W (1991) Epitope mapping by amino-acid-sequence-specific antibodies reveals that both ends of the α subunit of Na^+/K^+-ATPase are located on the cytoplasmic site of the membrane. Eur J Biochem 199: 195-202

Askari A and Huang W (1982) Na+, K+-ATPase: evidence for the binding of ATP to the phosphoenzyme. Biochem Biophys Res Commun 104: 1447-5

Axelsen KB and Palmgren MG (1998): Evolution of substrate specifities in the P-type ATPase superfamily. J Mol Evol 46: 84-101

Beggah AT, Jaunin P, Geering K (1997) J Biol Chem 227:10318-10326

Bilwes AM, Quezada CM, Croal LR, Crane BR, Simon MI (2001) Nucleotide binding to histidine kinase Chea. Nat Struct Biol 8:353

Bond H, Bader H, Post RL (1971) Acetyl phosphate as a substitute for ATP in (Na+K)-ATPase. Biochim Biophys Acta 241: 57-67

Bradford MM (1976) A rapid and sensitive method for the quantitation of microgram quantities of protein utilizing the principle of protein-dye binding. Anal Biochem 72: 248-254

Cavieres JD, Lilley KS, Ward DG (2000) Dissecting and mapping two nucleotide binding sites in Na,K ATPase. In Na/K ATPase and related ATPases (Taniguchi K and Kaya S, eds.), pp.115-122. Elsevier Science, Amsterdam.

Chapman R, Sidrauski C, Walter P (1998) Intracellular signaling from the endoplasmic reticulum to the nucleus. Annu Rev Cell Dev Biol 14: 459-85

Costa CJ, Gatto C, Kaplan JH (2003) Interactions between Na,K ATPase α-subunit ATP binding domains. J Biol Chem 278: 9176-9184

Daly SE, Blostein R, Lane LK (1997) Functional consequences of a posttransfection mutation in the H2-H3 cytoplasmic loop of the alpha subunit of Na,K-ATPase. J Biol Chem 272(10): 6341-7

Davis RL and Robinson JD (1988) Substrate sites of (Na+K)-ATPase: pertience of the adenine and fluorescein binding sites. Biochim Biophys Acta 953:26-36

Donnet C, Arystarkhova E, Sweadner KJ (2001) Thermal denaturation of the Na,K-ATPase provides evidence for alpha-alpha oligomeric interaction and gamma subunit association with the C-terminal domain. J Biol Chem 276: 7357-65

Dzhandzhugazyan KN and Modyanov NN (1994) Probing the α-subunitfolding by the dot-sandwich immunochemical analysis. In: The sodium pump. E. Bamberg, W. Schoner (eds), Steinkopff, Darmstadt, pp. 366-369

Eakle KA, Kabalin MA, Wang SG, Farley RA (1994) The influence of beta subunit structure on the stability of Na+/K(+)-ATPase complexes and interaction with K+. J Biol Chem 269: 6550-7

Ennis O, Maytum R and Mantle T (1997) Cloning and overexpression of rat kidney biliverdin IX alpha reductase as a fusion protein with glutathione S-transferase:

stereochemistry of NADH oxidation and evidence that the presence of the glutathione S-transferase domain does not effect BVR-A activity. Biochem. J 328: 33-36

Ettrich R, Melicherčík M, Teisinger J, Ettrichová O, Krumscheid R, Hofbauerová K, Kvasnička P, Schoner W, Amler E (2001) Three-dimensional structure of the large cytoplasmic H4-H5-loop of Na+/K+-ATPase deduced by restraint-based comparative modeling shows only one ATP-binding site, J. Mol. Model. 7: 184-192

Esmann M (1994) Influence of Na+ on conformational states in membrane-bound renal Na,K ATPase. Biochemistry 33: 8558-8565

Farley RA, Tran CM, Carilli CT, Hawke D, and Shively JE (1984) The amino acid sequence of a fluorescein-labeled peptide from the active site of (Na,K)-ATPase. J Biol Chem 259, 9532-9535

Garrahan PJ, Glynn IM (1967) The incorporation of inorganic phosphate into adenosine triphosphate by reversal of the sodium pump. J Physiol 192: 237-56

Gatto, C, Wang, AX, and Kaplan, JH (1998) The M4M5 cytoplasmic loop of the Na,K-ATPase, overexpressed in Escherichia coli, binds nucleoside triphosphates with the same selectivity as the intact native protein. J. Biol. Chem. 273: 10578-10585

Geering K (2001) The functional role of beta subunits in oligomeric P-type ATPases. J Bioenerg Biomembr 33: 425-438

Glynn IA (2002) A hundred years of sodium pumping. Annu Rev Physiol 64: 1-18

Hakansson KO (2003) The crystallographic structure of Na,K ATPase N-domain at 2.6Å resolution. J Mol Biol 332:1175-1182

Hasler U, Wang X, Crambert G, Beguin P, Jaisser F, Horisberger JD, Geering K (1998) Role of beta-subunit domains in the assembly, stable expression, intracellular routing, and functional properties of Na,K-ATPase. J Biol Chem 273: 30826-35

Haue L, Pedersen PA, Jorgensen PL, Hakansson KO (2003) Cloning, expression, purification and crystallization of the N-domain from α_2-subunit of the membrane-spanning Na,K ATPase protein. Acta Crystallogr D 59: 1259-1261

Heller H, Schaefer M, Schulten K, (1993) Molecular dynamics simulation of a bilayer of 200 lipids in the gel and in the liquid-crystal phases. J. Phys. Chem. 97:8343-60

Hilge M, Siegal G, Vuister GW, Guntert P, Gloor SM, Abrahams JP (2003) ATP-induced conformational changes of the nucleotide-binding domain of Na,K ATPase. Nat Struct Biol 10, 468-474

Hinz HR, Kirley TL (1990) Lysine 480 is an essential residue in the putative ATP site of lamb kidney (Na,K)-ATPase. Identification of the pyridoxal 5'-diphospho-5'-adenosine and pyridoxal phosphate reactive residue. J Biol Chem 265(18): 10260-5

Hiratsuka T, Sakata I, Uchida K (1973) Synthesis and properties of N6-(2, 4-dinitrophenyl)-adenosine 5'-triphosphate, an analogue of ATP. J Biochem (Tokyo) 74: 649-659

Hiratsuka T, Uchida K (1973a) Preparation and properties of 2'(or 3')-O-(2,4,6-trinitrophenyl) adenosine 5'-triphosphate, an analogue of adenosine triphosphate. Biochim Biophys Acta 320: 635-647

Hofbauerova K, Kopecky V, Etttrich R, Ettrichova O, Amler E (2002) Secondary and tertiary structure of nucleotide binding domain of α subunit of Na+K+ ATPase. Biopolymers 67: 242-246

Hofbauerova K, Kopecky V, Ettrich R, Kubala M, Teisinger J Amler E (2003) ATP binding is stabilized by a stacking interaction with the binding site of Na+/K+ ATPase. Biochem Biophys Res Commun 306: 416-420

Horisberger JD (2004) Recent Insights into the structure and Mechanism of the sodium pump. Physiology 19: 377-387

Huang W and Askari A (1975) (Na+K)-Activated adenosinetriphosphatase: fluorimetric determination of the associated K+-dependent 3-O-methylfluorescein phosphatase and its use for the assay of enzyme samples with low activities. Anal Biochem 66: 265-271

Imagawa T, Shunji K, Taniguch K (2003) The amino acid sequence 442GDASE446 in Na/K ATPase is an important motif in forming the high and low affinity ATP binding pockets. J Biol Chem 278:50283-92

Inturrisi CE and Titus E (1970) Ouabain-dependent incorporation of ^{32}P from p-nitrophenylphosphate into a microsomal phosphatase. Mol Pharmacol 6:99-107

Ivanov AV, Modyanov NN, Askari A (2002) Role of the self-association of beta subunits in the oligomeric structure of Na+/K+-ATPase. Biochem J 364: 293-9

Jorgensen PL (1975) Purification and characterization of (Na+, K+)-ATPase. V. Conformational changes in the enzyme Transitions between the Na-form and the K-form studied with tryptic digestion as a tool. Biochim Biophys Acta 401: 399-415

Jorgensen PL and Andersen JP (1988) J Membr Biol 103: 95-120

Jorgensen PL, Hakansson KO, Karlish SJD (2003) Structure and mechanism of Na,K ATPase: Functional sites and their interactions. Ann Rev Physiol 65:817-849

Kaplan JH (2002) Biochemistry of Na,K-ATPase. Annu Rev Biochem 71: 511-535

Karlish SJD (1980) Characterization of conformational changes in (Na,K)-ATPase labeled with fluorescein at the active site. J Bioenerget Biomembr 12:111-136

Kent RB, Emanuel JR, Ben Neriah Y, Levenson R, Housman DE (1987) Ouabain resistance conferred by expression of the cDNA for a murine Na+, K+-ATPase alpha subunit. Science 237(4817): 901-3

Kotyk A, Amler E (1995) Na,K-adenosinetriphosphatase: the paradigm of a membrane transport protein. Physiol Res 44: 261-74

Kotyk A (1998) Membrane transport: molecules involved. In: Structure and functions of biomembranes, 2nd English ed., Institute of Physiology, CzAcadSci, Prague, pp. 106-138

Kubala M, Hofbauerova K, Ettrich R, Kopecky V, Krumscheid R, Plasek J, Teisinger J, Schoner W and Amler E (2002) Phe475 and Glu446 but not Ser445 participate in ATP-binding to the α-subunit of Na+/K+ ATPase. Biochem Biophys Res Commun 297: 154-159

Kubala M, Plasek J, Amler E (2003) Limitations in linearized analyses of binding equilibria: binding of TNP-ATP to the H_4-H_5 loop of Na/K-ATPase. Eur Biophys J. 32(4): 363-369

Kubala M, Teisinger J, Ettrich R, Hofbauerova K, Kopecky V, Baumruk V, Krumscheid R, Plasek J, Schoner W and Amler E (2003a) Eight amino acids form the ATP recognition site of Na+/K+ ATPase. Biochemistry 42: 6446-6452

Kubala M, Plasek J, Amler E (2004) Fluorescence competition assay for the assesment of ATP binding to an isolated domain of Na+,K+ ATPase, Physiol Res 53(1):109-113

Kubala M, Obsil T, Obsilova V, Lansky Z, Amler E (2004a) Protein modeling combined with spectroscopic techniques: an attractive quick alternative to obtain structural information. Physiol Res 53:S187-S197

Kuster B, Shainskaya A, Pu HX, Goldshleger R, Blostein R, Mann M, Karlish SJ (2000)

A new variant of the gamma subunit of renal Na,K-ATPase. Identification by mass spectrometry, antibody binding, and expression in cultured cells. J Biol Chem 275: 18441-6

Lansky Z, Kubala M, Ettrich R, Kuty M, Plasek J, Teisinger J, Schoner W, Amler E (2004) The hydrogen bond between Arg423 and Glu472 and other key residues, Asp443, Ser477 and, Pro489, are responsible for the formation and different positioning of TNP-ATP and ATP within the nucleotide-binding site of Na+/K+ ATPase. Biochemistry 43: 8303-8311

Laskowski RA, McArthur MW, Moss DS, Thornton JM (1993) Procheck – a program to check the stereochemical quality of protein structures. J Appl Crystallogr 26: 283-291

Lemas MV, Hamrick M, Takeyasu K, Fambrough DM (1994) 26 amino acids of an extracellular domain of the Na,K-ATPase alpha-subunit are sufficient for assembly with the Na,K-ATPase beta-subunit. J Biol Chem 269: 8255-9

Linnertz H, Thonges D, Schoner W (1995) Na+/K+ ATPase with a blocked E1ATP site still allowes backdoor phosphorylation of the E2ATP site. Eur J Biochem 232: 420-424

Linnertz H, Kost H, Obsil T, Kotyk A, Amler E, and Schoner W (1998) Erythrosin 5' -isothiocyanate labels Cys549 as part of the low-affinity ATP binding site of Na+/K+-ATPase. FEBS Lett. 441, 103-5

Linnertz H, Urbanova P, Obsil T, Herman P, Amler E, Schoner W (1998a) Molecular distane measurements reveal an $(\alpha\beta)_2$ dimeric structure of Na+/K+ ATPase. High affinity ATP binding site and K+ -activated phosphatase reside on different alpha-subunits. J Biol Chem 273: 28813-21

Linnertz H, Lanz E, Gregor M, Antolovic R, Krumscheid R, Obsil T, Slavik J, Kovarik Z, Schoner W, Amler E (1999) Microenvironment of the high affinity ATP-binding site of Na+/K+-ATPase is slightly acidic. Biochem Biophys Res Commun 254(1): 215-21

Lutsenko S and Kaplan JH (1993) Biochemistry 32:6737-43

Lutsenko S, Kaplan JH (1994) Molecular events in close proximity to the membrane associated with the binding of ligands to the Na,K-ATPase. J Biol Chem 269(6): 4555-64

MacLennan DH, Brandl CJ, Korczak B, Green NM (1985) Nature 316:696-700

McDonough AA, Geering K, Farley RA (1990) The sodium pump needs its beta subunit. FASEB J 4: 1598-605

Moczydlowski EG, Fortes PA (1981a) Characterization of 2',3'-O-(2,4,6-trinitrocyclohexadienylidine)adenosine 5'-triphosphate as a fluorescent probe of the ATP site of sodium and potassium transport adenosine triphosphatase. Determination of nucleotide binding stoichiometry and ion-induced changes in affinity for ATP. J Biol Chem 256: 2346-2356

Moller JV, Juul B and le Maire M (1996) Structural organization, ion transport, and energy transduction of P-type ATPases. Biochim Biophys Acta 1286: 1-51

Morris GM, Goodsell D, Huey R, Olson AJ (1996) Distributed automated docking of flexible ligands to proteins: parallel application of AutoDock 2.4. J Comput-Aided Mol Des 10: 293-304

Obsil T, Merola F, Lewit-Bentley A, Amler E (1998) FEBS Lett 426:279-300

Ogawa H and Toyoshima C (2002) Homology modeling of the cation binding sites of the Na+/K+ ATPase. Proc Natl Acad Sci U S 99: 15977-15982

Patchornik G, Goldshleger R, Karlish SJ (2000) The complex ATP-Fe(2+) serves as a specific affinity cleavage reagent in ATP-Mg(2+) sites of Na,K-ATPase: altered ligation of Fe(2+) (Mg(2+)) ions accompanies the E(1)-->E(2) conformational change. Proc Natl Acad Sci U S A 97(22): 11954-9

Patchornik G, Munson K, Goldshleger R, Shainskaya A, Sachs G, Karlish SJ (2002) The ATP-Mg2+ binding site and cytoplasmic domain interactions of Na+,K+-ATPase investigated with Fe2+-catalyzed oxidative cleavage and molecular modeling. Biochemistry 41: 11740-9

Pedersen PA, Jorgensen JR, Jorgensen PL (2000) Importance of conserved alpha-subunit segment 709-GDGVND for Mg2+ binding, phosphorilation and energy transduction in Na,K ATPase. J Biol Chem 275: 37588-95

Price EM, Rice DA, Lingrel JB (1990) Structure-function studies of Na,K-ATPase. Site-directed mutagenesis of the border residues from the H1-H2 extracellular domain of the alpha subunit. J Biol Chem 265: 6638-41

Pu HX, Scanzano R, Blostein R (2002) Distinct regulatory effects of the Na,K-ATPase gamma subunit. J Biol Chem 277: 20270-6

Repke KR, Schon R (1973) Flip-flop model of (NaK)-ATPase function. Acta Biol Med Ger 31: Suppl:K19-30

Rice WJ, Young HS, Martin DW, Sachs JR and Stokes DL (2001) Structure of Na^+/K^+-ATPase at 11 Å resolution: Comparison with Ca^{2+}-ATPase in E_1 and E_2 states. Biophys J 80: 2187-2197

Robinson JD (1971) K^+-stimulated incorporation of ^{32}P from nitrophenyl phosphate into (Na+K)-activated ATPase preparation. Biochim Biophys Res Commun 42: 880-885

Robinson JD (1976) Substrate sites of the (Na+K)-ATPase. Biochim Biophys Acta 429: 1006-1019

Sali A and Blundell TL (1993) Comparative protein modeling by satisfaction of spatial restraints. J Mol Biol 234: 779-815

Scheiner-Bobis G, Schreiber S (1999) Glutamic acid 472 and lysine 480 of the sodium pump alpha 1 subunit are essential for activity. Their conservation in pyrophosphatases suggests their involvement in recognition of ATP phosphates. Biochemistry 38(29): 9198-208

Scheiner-Bobis G (2002) The sodium pump. Its molecular properties and mechanics of ion transport. Eur J Biochem 269: 2424-33

Schneider H, Scheiner-Bobis G (1997) Involvement of the M7/M8 extracellular loop of the sodium pump alpha subunit in ion transport. Structural and functional homology to P-loops of ion channels. J Biol Chem 272: 16158-65

Schultheis PJ, Wallick ET, Lingrel JB (1993) Kinetic analysis of ouabain binding to native and mutated forms of Na,K-ATPase and identification of a new region involved in cardiac glycoside interactions. J Biol Chem 268: 22686-94

Schuurmans Stekhoven F and Bonting SL (1981) Transport adenosine triphosphatases: properties and function. Physiol Rev 61: 1-76

Skou JC (1957) The influence of some cations on an adenosinetriphosphatase from periferal nerves. Biochim Biophys Acta 23: 394-401

Skou JC (1960) Further investigations on a $Mg^{++}+Na^{+}$-activated adenosinetriphosphatase, possibly related to the active, linked transport of Na^{+} and K^{+} across the nerve membrane. Biochim Biophys Acta 42: 6-23

Skou JC (1962) Preparation from mammalian brain and kidney of the enzyme system involved in active transport of Na^{+} and K^{+}. Biochim Biophys Acta 58: 314-325

Skou JC and Esmann M (1983) Effect of magnesium ions on the high-affinity binding of eosin to the (Na+K)-ATPase. Biochim Biophys Acta 727:101-107

Skou JC, Esmann M (1988) Eosin as a fluorescence probe for measurement of conformational states of Na+/K+ ATPase. Methods Enzymol 156:278-281

Smith DB and Johnson KS (1988) Single-step purification of polypeptides expressed in Escherichia coli as fusions with glutathione S-transferase. Gene 67: 31-37

Sorensen TLM, Moller JV and Nissen P (2004) Phosphoryl transfer and calcium ion occlusion in the calcium pump. Science 304: 1672-1675

Sweadner KJ and Rael E (2000) The FXYD gene family of small ion transport regulators of channels: cDNA sequence, protein signature sequence, and expression. Genomics 68: 41-56

Taniguchi K, Kaya S, Abe K, Mardh S (2001) The oligomeric nature of Na/K-transport ATPase. J Biochem (Tokyo) 129: 335-42

Teramachi S, Imagawa T, Kaya S, Taniguchi K (2002) Replacement of several single amino acid side chains exposed to the inside of the ATP-binding pocket induces different extents of affinity change in the high and low affinity ATP-binding sites of rat Na/K-ATPase. J Biol Chem 277: 37394-400

Thoenges D and Schoner W (1997) 2'-O-Dansyl analogs of ATP bind with high affinity to the low affinity ATP site of Na+/K+ ATPase and reveal the interaction of thwo ATP sites during catalysis. J Biol Chem 272:16315-21

Thoenges D, Amler E, Eckert T, Schoner W (1999) Tight binding of bulky fluorescent derivatives of adenosine to the low affinity E2ATP site leads to inhibition of Na+/K+ ATPase. Analysis of structural requirements of fluorescent ATP derivatives with a Koshland-Nemethy-Filmer model of two interacting ATP sites. J Biol Chem 274:1971-78

Thompson JD, Gibson TJ, Plewniak F, Jeanmougin F, Higgins DG (1997) The Clustal_X windows interface: flexible strategies for multiple sequence alignment aided by quality analysis tools. Nucleic Acids Res 25: 4876

Toyoshima C, Nakasako M, Nomura H, Ogawa H (2000) Crystal structure of the calcium pump of sarcoplasmic reticulum at 2.6 A resolution. Nature 405: 647-55

Toyoshima C, Nomura H (2002) Structural changes in the calcium pump accompanying the dissociation of calcium. Nature 418: 605-11

Toyoshima C and Inesi G (2004a) Structural basis of ion pumping by Ca2+ ATPase of the sarcoplasmatic reticulum. Annu Rev Biochem 73: 269-292

Toyoshima C and Mizutani T (2004) Crystal structure of the calcium pump with a bound ATP analogue. Nature 430: 529-535

Tran CM, Huston EE, Farley RA (1994a) Photochemical labeling and inhibition of Na,K-ATPase by 2-Azido-ATP. Identification of an amino acid located within the ATP binding site. J Biol Chem 269(9):6558-65

Tran CM, Scheiner-Bobis G, Schoner W, Farley RA (1994b) Identification of an amino acid in the ATP binding site of Na+/K(+)-ATPase after photochemical labeling with 8-azido-ATP. Biochemistry 33(14):4140-7

Tran CM, Farley RA (1996) Photoaffinity labeling of the active site of the Na+/K+ ATPase with 4-azido-2-nitrophenyl phosphate. Biochemistry 35: 47-55

Tran, CM and Farley RA (1999) Catalytic activity of an isolated domain of Na,K-ATPase expressed in Escherichia coli. Biophys. J. 77: 258-266

Vilsen B (1993) Glutamate 329 located in the fourth transmembrane segment of the alpha-subunit of the rat kidney Na+,K+-ATPase is not an essential residue for active transport of sodium and potassium ions. Biochemistry 32(48):13340-9

Vilsen B (1995) Mutant Glu781-->Ala of the rat kidney Na+,K(+)-ATPase displays low cation affinity and catalyzes ATP hydrolysis at a high rate in the absence of potassium ions. Biochemistry 34: 1455-63

Wang S, Taberno L, Zhang M, Harms E, Van Etten RL, Staufacher CV (2000) Crystal structure of low molecular weight protein tyrosine phosphatase from Saccharomyces Cerevisiae and its complex with the substrate p-nitrophenyl phosphate. Biochemistry 39: 1903-1914

Ward DG, Cavieres JD (1996) Binding of 2'(3')-O-(2,4-6-trinitrophenyl) ADP to soluble alpha beta protomers of Na, K-ATPase modified with fluorescein isothiocyanate. Evidence for two distinct nucleotide sites. J Biol Chem 271: 12317-21

Ward DG, Cavieres JD (1998) Affinity labeling of two nucleotide sites on Na,K ATPase using TNP-8N_3-[α-^{32}P]ADP photoactivable probe. Label incorporation before and after blocking the high affinity ATP site with fluorescein isothiocyanate. J Biol Chem 273:33759-65

12. Results Presentation

Publications

1) Lánský Z., Kubala M., Ettrich R., Kuty M., Plasek J., Teisinger J., Schoner W. and Amler E.: The hydrogen bond between Arg^{423} and Glu^{472} and another key residues Asp^{443}, Ser^{477} and Pro^{489} are responsible for forming and different positioning of TNP-ATP and ATP within the nucleotide binding site of Na^+/K^+-ATPase. Biochemistry 43: 8303-8311, 2004.

2) Krumscheid R., Ettrich R., Susankova K., Lansky Z., Hofbauerova K., Linnertz H., Teisinger J., Amler E. and Schoner W.: The phosphatase activity of the isolated H_4-H_5 loop of Na^+/K^+-ATPase resides outside of its ATP site. Eur. J. Biochem. 271, 3923-3936, 2004.

3) Kubala M., Obšil T., Obšilová V., Lánský Z. and Amler E.: Protein Modeling Combined with Spectroscopic Techniques: an Attractive Quick Alternative to Protein Crystallization. Physiological Research, 53, 109-113, 2004.

Posters

1) Kubala M., Lansky Z., Plasek J. and Amler E.: Novel methods for determination of AGE products and synovial fluid viscosity. Book of abstracts, 8th Conference on Methods and Applications of Fluorescence: Spectroscopy, Imaging and Probes, Prague, Czech Republic, 2003.

2) Lansky Z., Kubala M., Ettrich R., Kuty M., Plasek J., Teisinger J. and Amler E.: Arg^{423}, Glu^{472} and Pro^{489}; another residues supporting the structure of ATP binding site of the Na^+/K^+-ATPase. Eur. J. Biochem 271, Supplement 1, 2004; FEBS conference, Warsaw, 2004

3) Kubala M., Lansky Z., Ettrich R., Plasek J., Teisinger J. and Amler E.: Fluorescence studies of ATP-binding site of Na^+/K^+-ATPase. Eur. J. Biochem 271, Supplement 1, 2004; FEBS conference, Warsaw, 2004

4) Lansky Z., Kubala M., Ettrich R., Kuty M., Plasek J., Teisinger J. and Amler E.: The structure of the ATP-binding site of the Na^+/K^+-ATPase.Book of abstracts, The Annual Meeting of the Network of European Neuroscience Institutes, Prague, 2005

5)Simunova L., Kubala M., Lansky Z., Teisinger J. and Amler E.: Conformational changes of the Na^+/K^+-ATPase large cytoplasmatic loop induced by nucleotide binding. Book of abstracts, The Annual Meeting of the Network of European Neuroscience Institutes, Prague, 2005